

1

Characterization and Physical and Thermodynamic Properties of Oil Fractions

This chapter introduces the common methods for characterizing crude oils and petroleum fractions (i.e., oil fractions) and estimating their thermophysical properties. We begin by defining the essential bulk and fractional properties of oil fractions and by explaining the various types of distillation curves and their interconversion (Section 1.1.1). Next, we explain the generation of hypothetical components (“hypos”) or pseudocomponents of oil fractions based on boiling point ranges and the estimation of density and molecular weight distributions of the resulting hypos (Section 1.3). Sections 1.4–1.9 present six hands-on workshops using Excel spreadsheets and Aspen HYSYS Petroleum Refining for (1) the interconversion of distillation curve data; (2) the extrapolation of an incomplete distillation curve data; (3) the calculation of the mean average boiling point (MeABP) of a given oil fraction; (4) specifying an oil fraction in the *old* oil manager; (5) representing an oil fraction in the *new* petroleum assay manager; and (6) conversion from the oil manager to petroleum assay manager and improvements of the petroleum assay manager over the oil manager.

Section 1.10 introduces the essential thermophysical properties for developing refinery reaction and fractionation process models. Section 1.10.1 presents the useful methods for estimating the thermophysical properties (e.g., molecular weight, liquid density, critical properties, ideal gas heat capacity, and heat of vaporization) of pseudocomponents of oil fractions. Section 1.11 describes the important thermodynamic models for refinery reaction and fractionation processes. Section 1.12 discusses the estimation methods for other physical properties such as flash point, freeze point, and PNA (paraffin, naphthalene, and aromatic) content of a refinery feed. Section 1.13 summarizes the conclusion of this chapter. Finally, we present the nomenclature and bibliography.

1.1 Crude Assay

Crude oils and petroleum fractions are the most important feedstocks for refining processes. To properly simulate the refining processes, we must have good understanding of the compositional information and thermophysical properties of crude oils and petroleum fractions. However, the complexity of molecular composition of crude oils and petroleum fractions makes it hardly possible to

identify individual molecules. Instead, modern refiners use assay to characterize crude oils and petroleum fractions.

A typical crude assay includes two types of information for an oil sample: (1) *bulk properties* and (2) *fractional properties*. Table 1.1 provides examples of both types of properties of a crude assay. For design and modeling purposes, it is always the best practice to have process data obtained in the same period as assay data, as the properties and composition of crude change over time as it is produced from a given well. Kaes [1] suggested that the assay data should not be 2 years older than the process data used to build process simulation. We explain both bulk and fractional properties in the following sections.

1.1.1 Bulk Properties

Bulk properties include specific gravity, sulfur content, nitrogen content, metal (Ni, V, Fe, etc.) content, asphaltene content, C:H ratio, pour point, flash point, freeze point, smoke point, aniline point, cloud point, viscosity, carbon residue, light hydrocarbon yields (C1–C4), acid number, refractive index, and boiling point curve. We generally use the *API (American Petroleum Institute) gravity* to specify the specific gravity (SG) of the crude oil as

$$\text{API} = (141.5/\text{SG}) - 131.5 \quad (1.1)$$

or

$$\text{SG} = 141.5/(\text{API} + 131.5) \quad (1.2)$$

SG is the specific gravity defined as the ratio of the density of the crude oil to the density of water both at 15.6 °C (60 °F). The API gravity varies from less than 10 for very heavy crudes to between 10 and 30 for heavy crudes, to between 30 and 40 for medium crudes, and to above 40 for light crudes.

The *sulfur content* is expressed as a percentage of sulfur by weight and varies from less than 0.1% to greater than 5%. Crude oils with less than 1 wt% sulfur are called *low sulfur or sweet* and those with more than 1 wt% sulfur are called *high sulfur or sour*. Sulfur-containing constituents of the crude oil include simple mercaptans (also known as thiols), sulfides, and polycyclic sulfides. *Mercaptan sulfur* is simply an alkyl chain (R–) with –SH group attached to it at the end. The simplest form of R–SH is *methyl mercaptan*, CH₃SH.

The *pour point* is a measure of how easy or difficult it is to pump the crude oil, especially in cold weather. Specifically, the pour point is the lowest temperature at which a crude oil will flow or pour when it is chilled without disturbance at a controlled rate. The pour point of the whole crude or oil fractions boiling above 232 °C (450 °F) is determined by the ASTM test method D97.

The *flash point* of a liquid hydrocarbon or an oil fraction indicates its fire and explosion potential, and it is the lowest temperature at which sufficient vapor is produced above the liquid to form a mixture with air that a spontaneous ignition can occur if a spark is present. One of the standard ASTM test methods for flash point is D3278.

The *freeze point* is the temperature at which the hydrocarbon liquid solidifies at atmospheric pressure. It is an important property of kerosene and jet fuels

Table 1.1 A typical crude assay.

	Whole crude	C4 and C4-	C5-74 °C	74-166 °C	166-480 °C	480-249 °C	249-537 °C	537 °C+
Cut volume, %	100	1.57	8.26	20.96	17.11	17.52	24.71	9.87
API gravity	38.6	117.9	80.6	55.7	42.82	34.7	25.5	10.9
Carbon, wt%		82.5	83.9	86.0	86.1	86.4	86.4	
Hydrogen, wt%		17.5	16.1	14.0	13.9	13.2	12.8	
Pour point, °C	-12.2				-53.9	-10.6	38.9	56.7
Sulfur, wt%	0.3675			0.0137	0.058	0.2606	0.6393	1.1302
Nitrogen, ppm	970	0	0	0	2.4	94.6	1346	4553
Viscosity at 20 °C/68 °, cSt	4.59	0.41	0.46	0.73	1.74	6.76	118.4	1789.683
Viscosity at 100 °C/212 °, cSt	1.35	0.24	0.26	0.38	0.68	1.43	5.91	372
Mercaptan sulfur, ppm	25			22.8	35.3			
CCR, wt%	1.71					0	0.11	14.21
Nickel, ppm	1.7					0	0.1	12.8
Vanadium, ppm	5.2					0	0.1	41.5
Heat of combustion (gross), BTU/lb	19701							
Heat of combustion (net), BTU/lb	18496	19078	18729	18561	18546			
Salt content, ptb	1.7							
Paraffins, vol%		100	84.77	46.64	48.83	39.42	30.18	
Naphthenes, vol%		0	13.85	36.56	31.54	37.44	31.83	
Aromatics, vol%				16.8	15.15			
Freeze point, °C					-43.9	-0.6		
Smoke point, mm					23.3			
Cetane index 1990 (D4737)	37	131	44	30	43	55	59	43
Cloud point, °C					-47.8	-3.9		

(Continued)

Table 1.1 (Continued)

	Whole crude		C4 and C4-	C5-74 °C	74-166 °C	166-480 °C	480-249 °C	249-537 °C	537 °C+
Aniline point, °C						57.7	69.5	87.1	
Distillation type	D1160	D86	D86	D86	D86	D86	D86	D1160	D1160
ASTM IBP, °C	0.2	-70.9	-57.2	206.9	97.2	263.1	263.1	365.2	559.1
5 vol%, °C	51.9	-27.3	-32.9	212.1	100.1	265.6	265.6	367.8	561.7
10 vol%, °C	79.7	13.8	-10.1	214.8	101.6	266.7	266.7	373.1	565.7
20 vol%, °C	119.9	30.2	-1.0	220.8	104.9	269.7	269.7	384.1	575.1
30 vol%, °C	160.7	36.8	2.7	227.6	108.7	273.7	273.7	396.7	585.8
40 vol%, °C	205.6	38.2	3.4	235.8	113.2	278.4	278.4	410.8	598.2
50 vol%, °C	254.3	38.3	3.5	244.1	117.8	283.2	283.2	426.3	612.4
60 vol%, °C	308.7	42.7	5.9	254.1	123.4	288.7	288.7	442.8	631.2
70 vol%, °C	364.0	46.5	8.1	265	129.4	294.8	294.8	459.5	653.1
80 vol%, °C	425.6	49.3	9.6	276.8	136.0	301.4	301.4	477.6	681.3
90 vol%, °C	502.9	47.5	8.6	289.4	143.0	308.3	308.3	496.0	718.7
95 vol%, °C	570.9	47.1	8.4	296.4	146.9	312.2	312.2	507.4	751.0
ASTMEBP, °C	730.7	47.9	8.8	307.7	153.2	318.2	318.2	520.7	791.6

because of the very low temperatures encountered at high altitudes in jet planes. A standard test method for the freeze point is ASTM D4790.

The *smoke point* refers to the height of a smokeless flame of fuel in millimeters beyond which smoking takes place. It reflects the burning quality of kerosene and jet fuels and is determined by ASTM D1322.

The *aniline point* represents the minimum temperature for complete miscibility of equal volumes of aniline and petroleum oil. It is an important property of diesel fuels and is measured by ASTM D611.

The *cloud point* refers to the temperature at which solidifiable components (waxes) present in the oil sample begin to crystallize or separate from solution under a method of prescribed chilling. It is an important specification of middle distillate fuels, as determined by ASTM D2500.

The *Conradson carbon residue (CCR)* results from ASTM D189. It measures the coke-forming tendencies of oil. It is determined by destructive distillation of a sample to elemental carbon (coke residue) in the absence of air, expressed as the weight percentage of the original sample. A related measure of the carbon residue is called *Ramsbottom carbon residue*, as determined by ASTM D524-15. A crude oil with a high CCR has a low value as a refinery feedstock.

The *acid number* results from ASTM D3339-11 that determines the organic acidity of a refinery stream.

The *refractive index* represents the ratio of the velocity of light in a vacuum to that in the oil. It is determined by ASTM D1218.

The *gross heat of combustion or high heating value (HHV)* is the amount of heat produced by the complete combustion of a unit quantity of fuel. We obtain the gross heat of combustion by cooling down all products of the combustion to the temperature before the combustion and by condensing all the water vapor formed during combustion.

The *net heat of combustion or lower heating value (LHV)* is obtained by subtracting the latent heat of vaporization of the water vapor formed by combustion from the gross heat of combustion or higher heating value.

The *true boiling point (TBP) distillation* [1] of a crude oil or petroleum fractions results from using the US Bureau of Mines Hempel method and ASTM D285. Neither of these methods specifies the number of theoretical stages or the molar reflux ratio used in the distillation. Consequently, there is a trend toward applying a 15.5 distillation according to ASTM D2892, instead of the TBP. The 15.5 distillation uses 15 theoretical stages and a molar reflux ratio of 5.

A key result from a distillation test is the *boiling point curve*, that is, the boiling point of the oil fraction versus the fraction of oil vaporized. The *initial boiling point (IBP)* is the temperature at which the first drop of liquid leaves the condenser tube of the distillation apparatus. The final boiling point or the *end point (EP)* is the highest temperature recorded in the test.

In addition, oil fractions tend to decompose or crack at a temperature of approximately 650 °F (344 °C) at 1 atm. Thus, the pressure of TBP distillation is gradually reduced to as low as 40 mmHg, as this temperature is approached to avoid cracking of the sample and distorting the measurements of true components in the oil.

The TBP distillation typically takes much time and labor. In practice, we carry out the distillation test of oil fractions using other less costly ASTM methods and convert the resulting boiling point curve into TBP curve using correlations, as given in the *API Technical Data Book – Petroleum Refining* [2]. We have implemented these correlations in an Excel spreadsheet, *ASTMConvert.xls*, for the interconversion of boiling point curves from typical ASTM distillation methods in a hands-on workshop in Section 1.4.

The *ASTM D86 distillation* of an oil fraction takes place at laboratory room temperature and pressure. Note that the D86 distillation will end below an approximate temperature of 650 °F (344 °C), at which petroleum oils begin to crack at 1 atm.

The *ASTM D1160 distillation* of an oil fraction is applicable to high-boiling oil samples (e.g., heavy heating oil, cracker gas oil feed, and residual oil) for which there is a significant cracking at atmospheric pressures. The sample is distilled at a reduced pressure, typically at 10 mmHg, to inhibit cracking. In fact, at 10 mmHg, we can distill an oil fraction up to temperatures of 950–1000 °F (510–538 °C), as reported on a 760 mmHg basis. The reduced pressure used for D1160 distillation produces a separation of components that is more ideal than that for D86 distillation.

The *ASTM D2887 distillation* of an oil fraction is a popular chromatographic procedure to “simulate” or predict the boiling point curve of an oil fraction. We determine the boiling point distribution by injecting the oil sample into a gas chromatograph that separates the hydrocarbons in a boiling point order. We then relate the retention time inside the chromatograph to the boiling point through a calibration curve.

1.1.2 Fractional Properties

Bulk properties provide a quick understanding of the type of the oil sample such as sweet and sour, and light and heavy. However, refineries require *fractional properties* of the oil sample that reflects the property and composition for a specific boiling point range to properly refine it into different end products such as gasoline, diesel, and raw materials for chemical process. Fractional properties usually contain PNA contents, sulfur content, and nitrogen content for each boiling point range; octane number for gasoline; freezing point; cetane index; and smoke point for kerosene and diesel fuels.

The *octane number* is a measure of the knocking characteristics of a fuel in a laboratory gasoline engine according to ASTM D2700 [1]. We determine the octane number of a fuel by measuring its knocking value compared to the knocking of a mixture of *n*-heptane and isooctane or 2-2-4-trimethylpentane (224TMP). By definition, we assign an octane number of 0 to pure *n*-heptane and of 100–224TMP. Therefore, a mixture of 30% heptanes and 70% isooctane has an octane number of 70.

There are two specific octane numbers in use. The *motor octane number* (MON) reflects the engine performance at highway conditions with high speeds (900 rpm), whereas the *research octane number* (RON) corresponds to the low-speed city driving (600 rpm). RON is typically higher than MON because of engine test efficiencies. The posted octane number is an average of MON and RON.

The *cetane number* measures the ease for self-ignition of a diesel fuel sample and is essentially an opposite of the octane number. It represents the percentage of pure cetane (*n*-hexadecane) in a blend of cetane and alpha-methylnaphthalene that matches the ignition quality of a diesel fuel sample. This quality is important for middle distillate fuels.

The *cetane index* is a substitute for the cetane number of diesel fuel. It is calculated based on the fuel’s specific gravity and distillation range using ASTM methods D976 and D4737.

1.1.3 Interconversion of Distillation Curves

While building a refining process simulation, the distillation curve of the oil sample is the most confusing information among assay data, as different methods are used to obtain volatility characteristics of an oil sample. The most widely used tests of distillation curve are ASTM D86, ASTM D1160 (atmospheric distillation), ASTM D1160 (vacuum distillation), ASTM D2887 (chromatographic simulation), and TBP. API Technical Databook [2] presents the characteristics of each test and gives the correlations to perform interconversion among these ASTM distillation types. Most commercial process simulators include the capability to convert one type of distillation curve into the other. We develop an MS Excel spreadsheet, which automates the API conversion between any two of the ASTM distillation types (see Figure 1.1). Section 1.4 presents a hands-on workshop for this interconversion of distillation curve data.

760 mmHg ASTM-D86 (C)	Vol %	760 mmHg ASTM-D86 (F)	760 mmHg TBP (°F)	760 mmHg TBP (C)	760 mmHg TBP (C)	760 mmHg TBP (F)	760 mmHg ASTM-D86 (F)	760 mmHg ASTM-D86 (C)
160.0	0%	320	259.1	126.2	126.2	258.1	320	160.0
176.7	10%	350	316.5	158.1	158.1	316.5	350	176.7
193.3	30%	380	372.9	189.2	189.2	372.6	380	193.3
206.7	50%	404	411.2	210.7	210.7	411.2	404	206.7
222.8	70%	433	451.2	232.9	232.9	451.2	433	222.8
242.8	90%	469	496.7	258.2	258.2	496.7	469	242.8
248.9	100%	480	503.3	261.7	261.7	503.0	480	248.9
ASTM-D2887 (C)	Wt%Vol%	ASTM-D2887 (F)	760 mmHg TBP (°F)	760 mmHg TBP (C)	760 mmHg TBP (C)	760 mmHg TBP (F)	ASTM-D2887 (F)	ASTM-D2887 (C)
145.0	5%	293	322.2	161.2	348.0	658.4	639.1711023	337.3
151.7	10%	305	327.7	164.3	369.0	696.2	685.3443333	363.0
162.2	30%	324	332.4	166.9	406.0	762.8	756.2204757	402.3
168.9	50%	336	336.3	168.9	433.0	811.4	811.4	433.0
173.3	70%	344	339.8	170.9	459.0	852.2	861.2301007	460.7
181.7	90%	359	350.1	176.7	455.0	923.0	922.5542047	494.8
187.2	95%	369	357.4	180.8	512.0	953.6	974.5478925	523.6
198.9	100%	390	366.2	185.7	556.0	1032.8	1038.378625	559.1
ASTM-D2287 (C)	Wt%Vol. %	ASTM-D2287 (F)	760 mmHg ASTM-D86 (F)	760 mmHg ASTM-D86 (C)	760 mmHg ASTM-D86 (C)	760 mmHg ASTM-D86 (F)	ASTM-D2287 (F)	ASTM-D2287 (C)
25.0	0%	77	121.3	49.6	258.8	568.9	446.4892018	230.3
33.8	10%	93	128.2	53.5	349.7	661.5	665.3731877	318.5
64.4	30%	148	154.3	68.2	352.0	737.5	715.3377437	379.6
101.7	50%	215	206.3	98.8	424.2	795.5	787.7262099	419.8
140.6	70%	285	270.5	132.5	459.0	852.2	856.5298061	458.1
182.2	90%	360	334.3	167.8	514.5	958.0	964.7774337	518.2
208.9	100%	408	367.5	186.4	577.9	1072.2	1273.441992	689.7
760 mmHg ASTM-D1160 (C)	Vol%	760 mmHg ASTM-D1160 (F)	760 mmHg TBP (°F)	760 mmHg TBP (C)	760 mmHg TBP (C)	760 mmHg TBP (F)	760 mmHg ASTM-D1160 (F)	760 mmHg ASTM-D1160 (C)
369.0	10%	696.2	686.2	363.4	143.1	289.5	300.1	149.0
406.0	30%	762.3	757.9	403.3	201.5	394.7	400.1	204.5
433.0	50%	811.4	811.4	433.0	246.1	475.0	475.0	246.1
459.0	70%	858.2	857.3	458.8	287.7	549.9	550.0	287.8
495.0	90%	923	922.5	494.7	343.3	650.0	650.0	343.4

Figure 1.1 Conversion spreadsheet for distillation curves.

1.2 Boiling Point-Based Hypothetical or Pseudocomponent Generation

To simulate refining processes, the first task is to construct a hypothetical (hypo) or pseudocomponent scheme to characterize the feedstock. Data requirement and definition of the hypos or pseudocomponents depend on the type of the refining process to be modeled. There are different issues to consider when specifying hypos for fractionation and reaction units.

The hypos for fractionation units have to accurately characterize volatilities of the hydrocarbons in the feedstock in order to calculate the vapor–liquid equilibrium in distillation columns. Therefore, refiners use hypos based on boiling point ranges to represent the feedstock and model fractionation units. For modeling of reaction units, refiners partition the hydrocarbons into multiple lumps (or model compounds) based on molecular structure or/and boiling point ranges and assume the hydrocarbons of each lump to have an identical reactivity in order to develop the reaction kinetics for reaction units.

This section deals with hypo or pseudocomponent generation based on boiling point ranges for fractionation units. Chapters 4–7 will represent the hypo schemes for the major reaction units in modern refinery – fluid catalytic cracking (FCC) unit, catalytic reformer, catalytic hydrocracker, delayed coker, and alkylation unit.

Most commercial process simulators include the capability to generate hypos based on boiling point ranges representing the oil fractions. Workshop 1.4 in Section 1.7 demonstrates how to use Aspen HYSYS to generate hypos based on boiling point ranges for a given oil fraction with required analysis data.

Specifically, there are four steps to develop pseudocomponents based on boiling point ranges to represent petroleum fraction.

- 1) Convert ASTM D86/ASTM D1160/ASTMD2887 into TBP curve if TBP curve is not available.
 - We develop a spreadsheet, *ASTMConvert.xls*, that allows interconversion between different ASTM distillation types based on the correlations from [2] (see Figure 1.1).
- 2) Cut the entire boiling point range into a number of cut point ranges, which are used to define pseudocomponents (see Figure 1.2).
 - The determination of number of cuts is arbitrary. Table 1.2 provides the typical boiling point widths for pseudocomponents in commercial process simulators.
- 3) Estimate the density distribution of pseudocomponents if only the bulk density is available.
 - Assume the UOP or Watson–Murphy “characterization factor” or K factor to be constant throughout the entire boiling point range and calculate the mean average boiling point (MeABP). Dissimilar to weight average boiling point (WABP), MeABP is defined as the average of molal average boiling

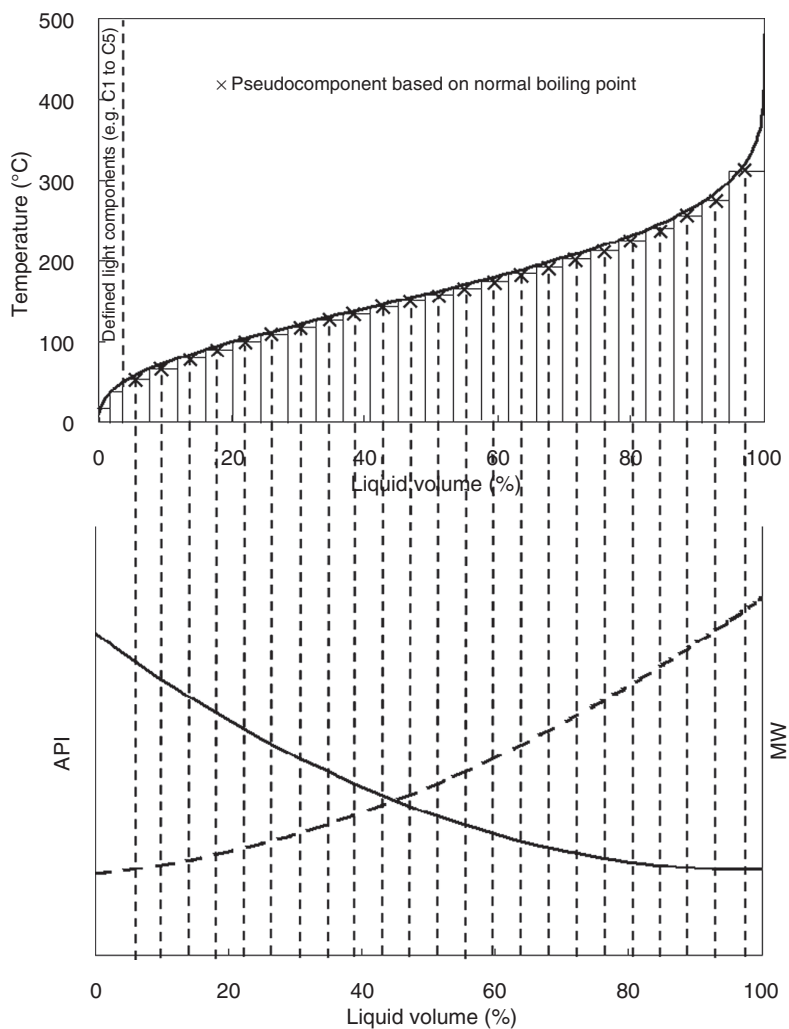


Figure 1.2 Relationship between pseudocomponent properties and the TBP curve. (Redraw from [1].)

Table 1.2 Typical boiling point widths for pseudocomponents in commercial process simulators.

Boiling point range	Suggested number of pseudocomponents
IBP–800 °F (425 °C)	30
800–1200 °F (650 °C)	10
1200–1650 °F (900 °C)	8

point (MABP) and cubic average boiling point (CABP). The following equations define these four boiling point indicators:

$$\text{WABP} = \sum_{i=1}^n x_i T_{bi} \quad (1.3)$$

$$\text{MABP} = \sum_{i=1}^n x_i T_{bi} \quad (1.4)$$

$$\text{CABP} = \left(\sum_{i=1}^n x_i T_{bi}^{1/3} \right)^3 \quad (1.5)$$

$$\text{MeABP} = \frac{\text{MABP} + \text{CABP}}{2} \quad (1.6)$$

where T_{bi} indicates the boiling point of component i and x_i in Eqs. (1.3)–(1.5) indicates weight fraction, molar fraction, and volume fraction of component i , respectively. Here, we create a spreadsheet tool (see Figure 1.3) to perform the iteration of estimating MeABP based on the methods presented by Bollas *et al.* [3] (see Section 1.5)

$$K_{\text{avg}} = [\text{MeABP}]^{0.333} / \text{SG}_{\text{avg}} \quad (1.7)$$

where K_{avg} is the Watson K factor and SG_{avg} is the bulk specific gravity $60^\circ\text{F}/60^\circ\text{F}$.

- Calculate the density distribution of the entire boiling point range.

$$\text{SG}_i = [T_{i,b}]^{0.333} / K_{\text{avg}} \quad (1.8)$$

where SG_i is the specific gravity $60^\circ\text{F}/60^\circ\text{F}$ of pseudocomponent i and $T_{i,b}$ is the normal boiling point of pseudocomponent i .

- 4) Estimate molecular weight distribution of the entire boiling point range if not available and required properties for modeling purpose (see Section 1.4 for details).

Lacking the analysis data of high boiling point range ($>570^\circ\text{C}$) is a common problem while building pseudocomponents based on boiling point ranges. Therefore, we need to extrapolate the incomplete distillation curve in order to cover the entire boiling point range. Least squares and probability distribution functions are most widely used to perform the extrapolation of distillation curve in most commercial process simulators. Sanchez *et al.* [5] presented a comprehensive review of using probability distribution functions to fit distillation curves of petroleum fraction. They conclude that the cumulative beta function (with four parameters) can represent a wide range of petroleum products. The beta cumulative density function is

$$f(x, \alpha, \beta, A, B) = \int_A^{x \leq B} \left(\frac{1}{B-A} \right) \frac{\Gamma(\alpha + \beta)}{\Gamma(\alpha)\Gamma(\beta)} \left(\frac{x-A}{B-A} \right)^{\alpha-1} \left(\frac{B-x}{B-A} \right)^{\beta-1} \quad (1.9)$$

where α and β refer to the positive-valued parameters that control the shape of the distribution and Γ refers to the standard gamma function, which is an extension of the factorial function, with its argument shifted down by 1 to real and

	A	B	C	D
4	TBP Curve @ 760 mmHg			
5	Vol%	Temperature (F)		Initial
6	0	256.8		0
7	10	368.2		5
8	30	447.2		10
9	50	516.9		15
10	70	583.9		20
11	90	633.4		25
12	100	722.2		30
13				35
14	Specific gravity	0.8505		40
15	Refractive index @ 20 C			45
16	Oxygen content (wt%)	0.00		50
17	Initial MeABP (F) [Enter as first guess in yellow cell]	506.76		55
18				60
19	Trial MeABP (F)	497.46		65
20	Trial MeABP (R)	957.13		70
21	Watson-K	11.59		75
22				80
23	Calc. VABP (R)	969.22		85
24	Calc. WABP (R)	972.98		90
25	Calc. MABP (R)	948.85		95
26	Calc. CABP (R)	965.42		
27				
28	Calc. MeABP (R)	957.13		
29				
30	Error (Trial MeABP - Calc. MeABP)	0.00000	(Use goalseek to drive	
31				
32	Correlation for refractive index	A	B	C
33	Naphthas	1.028	0.53	
34	Straight or hydrosulfurized gas oils	0.9734	0.59	
35	Deeply hydrogenated fractions	0.9713	0.59	
36	Short residues	0.9345	0.63	0.006
37	FCC feeds	0.8995	0.60	0.006
38	Coal liquids	0.8995	0.60	0.006
39	Stream cracker residue			
40				
41	Selected correlation			
42				
43				

Figure 1.3 Iteration spreadsheet for MeABP calculation.

complex numbers. That is, if ν is a positive integer, then $\Gamma(\nu) = (\nu - 1)!$ A and B parameters set lower and upper bounds on the distribution and x represents normalized recovery. We develop an MS Excel spreadsheet, *Beta.xls*, to perform the extrapolation of distillation curve by using the cumulative beta distribution function (see Figure 1.4).

Section 1.5 presents Workshop 1.2 for applying our spreadsheet to extrapolate an incomplete distillation curve. We note that we should use the density distribution together with the boiling point whenever the density distribution is available (in step 3), because the assumption of constant Watson K factor always fails in low and high boiling point ranges of the distillation curve. Figure 1.5 compares the pseudocomponents generated from constant Watson K factor and from density distribution. Using a constant Watson K factor shows significant deviations from assay data on estimating the densities of pseudocomponents, particularly in both

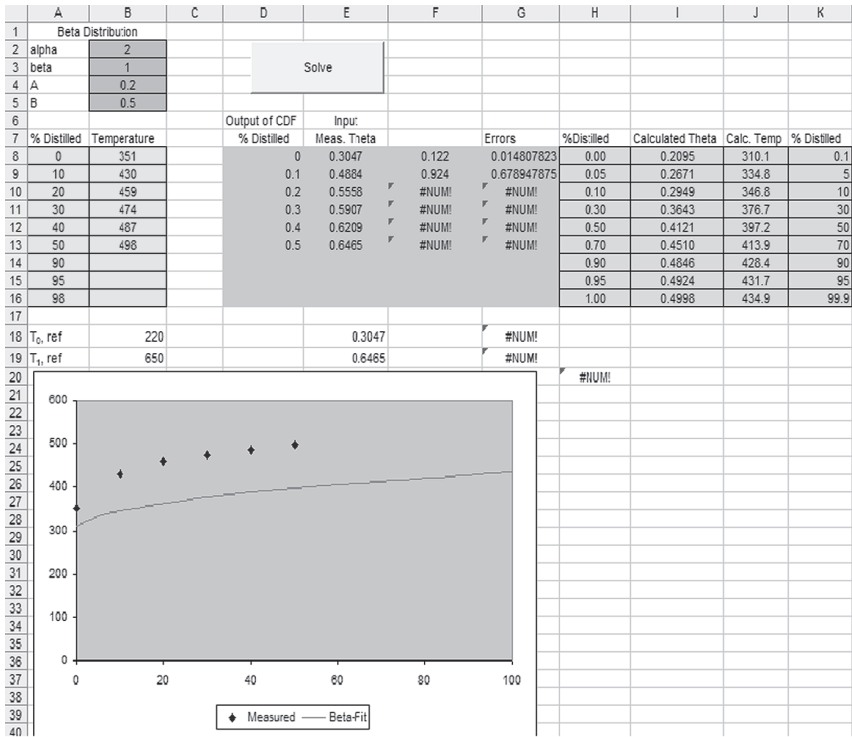


Figure 1.4 Spreadsheet for extrapolating distillation curve.

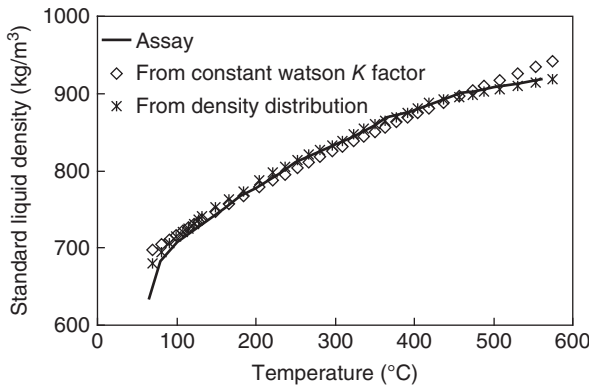


Figure 1.5 Comparison of the pseudocomponents generated from constant Watson K factor and density distribution. (Adapted from Kaes 2000 [1].)

light and heavy ends of the distillation curve. On the other hand, using the density distribution is able to provide good estimation of the densities of pseudocomponents. Estimating the densities of pseudocomponents is the most important part when developing pseudocomponents because density is required for most physical property estimations.

1.3 Workshop 1.1 – Interconvert Distillation Curves

There are two situations that we may encounter when the distillation curve available is not a TBP curve and needs to be converted: (1) it is another ASTM type, and (2) it is ASTM D1160 at vacuum pressure. The spreadsheet we have developed is able to solve these two cases. The following steps demonstrate how to convert an ASTM D1160 curve (at 10 mmHg) into a TBP curve.

- Step 1.* Open *WS1.1 ASTMConvert.xls* (Figure 1.6).
- Step 2.* Copy and paste the ASTM D1160 curve into the sheet for interconversion among different testing pressures of ASTM D1160 (Figure 1.7).
- Step 3.* Input the testing pressure, which is 10 mmHg in this case (Figure 1.8).
- Step 4.* The blue cells will show the converted results, which correspond to ASTM D1160 at 1 atm (Figure 1.9).
- Step 5.* Copy the values of ASTM D1160 (at 1 atm) to the sheets for converting ASTM D1160 at 1 atm into TBP (Figure 1.10).
- Step 6.* The blue cells reveal the converted TBP curve (Figure 1.11).

1.4 Workshop 1.2 – Extrapolate an Incomplete Distillation Curve

- Step 1.* Open *WS1.2 Beta.xls*. Purple cells show the adjustable parameters in beta distribution function, yellow cells require the input of the distillation curve, tan cells and the graph indicate the fitted results (Figure 1.12).
- Step 2.* Input the incomplete distillation curve into yellow cells. The user is allowed to add/remove the cells of “% Distilled” and “Temperature” according to the number of points in distillation curve (Figure 1.13).
- Step 3.* Click “solve” to run the fitting program (Figure 1.14).
- Step 4.* The purple cells show the fitted parameters. The tan cells and the graph represent the extrapolated distillation curve (Figure 1.15).

1.5 Workshop 1.3 – Calculate MeABP of a Given Assay

- Step 1.* Open *WS1.3 MeABP Iteration.xls* (Figure 1.16).
- Step 2.* Select type of the oil fraction. We choose naphtha in this case (Figure 1.17).
- Step 3.* Input TBP curve and specific gravity in blue cells (Figure 1.18).
- Step 4.* Go to Tool/Goal Seek (for new version of Excel, Data → What-If Analysis → Goal Seek) (Figure 1.19).
- Step 5.* Assign yellow cell to “By changing cell” and green cell to “Set cell” and input “0” in “To value.” And then, click “OK” (Figure 1.20).
- Step 6.* The yellow cell reveals the calculated MeABP for the given oil fraction (Figure 1.21).

Pressure =	30	mmHg	2 =< P =< 760			
X	0.00180742			760 mmHg	760 mmHg	760 mmHg
TBP/D1160 (C)	Vol%	TBP/D1160 (F)	TBP/D1160 (R)	TBP/D1160 (R)	TBP/D1160 (F)	TBP/D1160 (C)
143.1	10%	289.5	749.2	941.7	482.1	250.0
201.5	30%	394.7	854.4	1063.5	603.8	317.7
246.1	50%	475.0	934.7	1154.8	695.1	368.4
287.7	70%	549.9	1009.6	1238.8	779.1	415.1
343.3	90%	650.0	1109.7	1349.2	889.5	476.4

Figure 1.7 Input cells of ASTM D1160 interconversion in ASTMConvert.xls.

47	Pressure =	10	mmHg	2 =< P =< 760			
48	X	0.00195599			760 mmHg	760 mmHg	760 mmHg
49	TBP/D1160 (C)	Vol%	TBP/D1160 (F)	TBP/D1160 (R)	TBP/D1160 (R)	TBP/D1160 (F)	TBP/D1160 (C)
50	143.1	10%	289.5	749.2	997.0	537.4	280.8
51	201.5	30%	394.7	854.4	1122.8	663.1	350.6
52	246.1	50%	475.0	934.7	1216.6	756.9	402.7
53	287.7	70%	549.9	1009.6	1302.6	842.9	450.5
54	343.3	90%	650.0	1109.7	1415.1	955.5	513.0

Figure 1.8 Input pressure for ASTM D1160 interconversion.

47	Pressure =	10	mmHg	2 =< P =< 760			
48	X	0.00195599			760 mmHg	760 mmHg	760 mmHg
49	TBP/D1160 (C)	Vol%	TBP/D1160 (F)	TBP/D1160 (R)	TBP/D1160 (R)	TBP/D1160 (F)	TBP/D1160 (C)
50	143.1	10%	289.5	749.2	997.0	537.4	280.8
51	201.5	30%	394.7	854.4	1122.8	663.1	350.6
52	246.1	50%	475.0	934.7	1216.6	756.9	402.7
53	287.7	70%	549.9	1009.6	1302.6	842.9	450.5
54	343.3	90%	650.0	1109.7	1415.1	955.5	513.0

Figure 1.9 Results of ASTM D1160 interconversion.

37	760 mmHg		760 mmHg	760 mmHg	760 mmHg
38	ASTM-D1160 (C)	Vol%	ASTM-D1160 (F)	TBP (F)	TBP (C)
39	280.8	10%	537.3541391	527.3	275.2
40	350.6	30%	663.1131895	657.8	347.7
41	402.7	50%	756.9327522	756.9	402.7
42	450.5	70%	842.8909373	842.9	450.5
43	513.0	90%	955.4507826	955.6	513.1

Figure 1.10 Input cells for other ASTM interconversion in ASTMConvert.xls.

37	760 mmHg		760 mmHg	760 mmHg	760 mmHg
38	ASTM-D1160 (C)	Vol%	ASTM-D1160 (F)	TBP (F)	TBP (C)
39	280.8	10%	537.3541391	527.3	275.2
40	350.6	30%	663.1131895	657.8	347.7
41	402.7	50%	756.9327522	756.9	402.7
42	450.5	70%	842.8909373	842.9	450.5
43	513.0	90%	955.4507826	955.6	513.1

Figure 1.11 Result cells for other ASTM interconversion in ASTMConvert.xls.

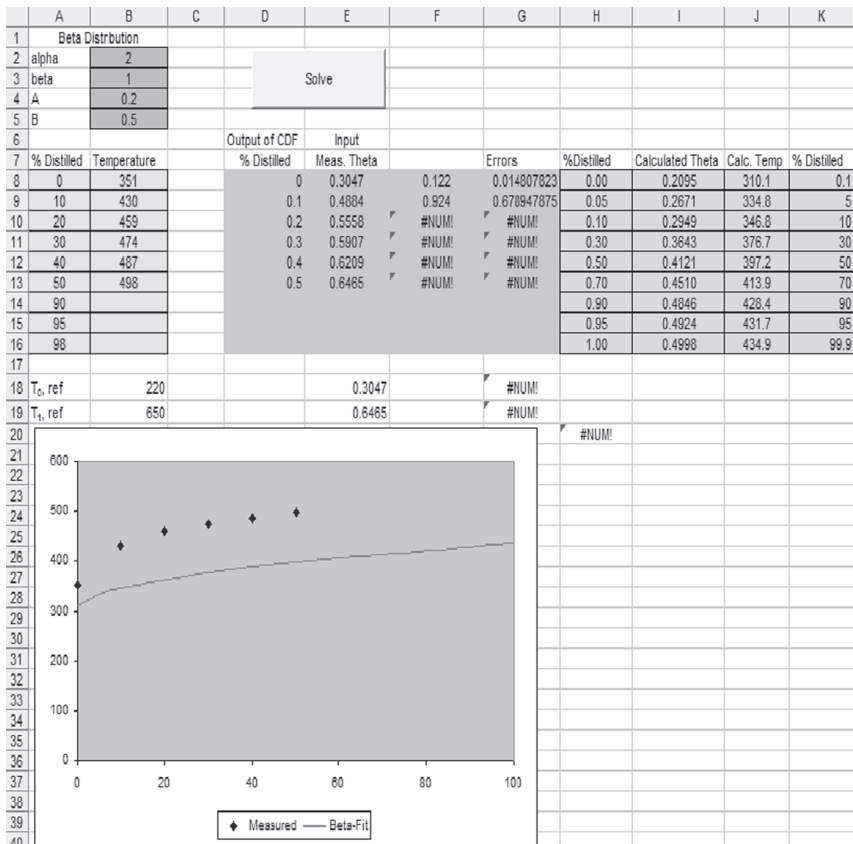


Figure 1.12 WS1.2 Beta.xls.

1.6 Workshop 1.4 – Represent an Oil Fraction by the Old Oil Manager in Aspen HYSYS Petroleum Refining

- Step 1. Start a new case in Aspen HYSYS Petroleum Refining and save as *WS1.4 Oil Manager.hsc* (Figure 1.22).
- Step 2. Click “add” to add a new component list (Figure 1.23).
- Step 3. Click “view” to edit the component list. Add light components, which are shown in assay data (Figure 1.24).
- Step 4. Click “add” in “fluid pkgs” tab to add the thermodynamic model (Figure 1.25).
- Step 5. Select the Peng–Robinson method (Figure 1.26).
- Step 6. Click “Input Assay” in “Oil Manager” environment (Figure 1.27).
- Step 7. Add an assay by inputting the TBP curve, bulk density, and light end composition (Figure 1.28).

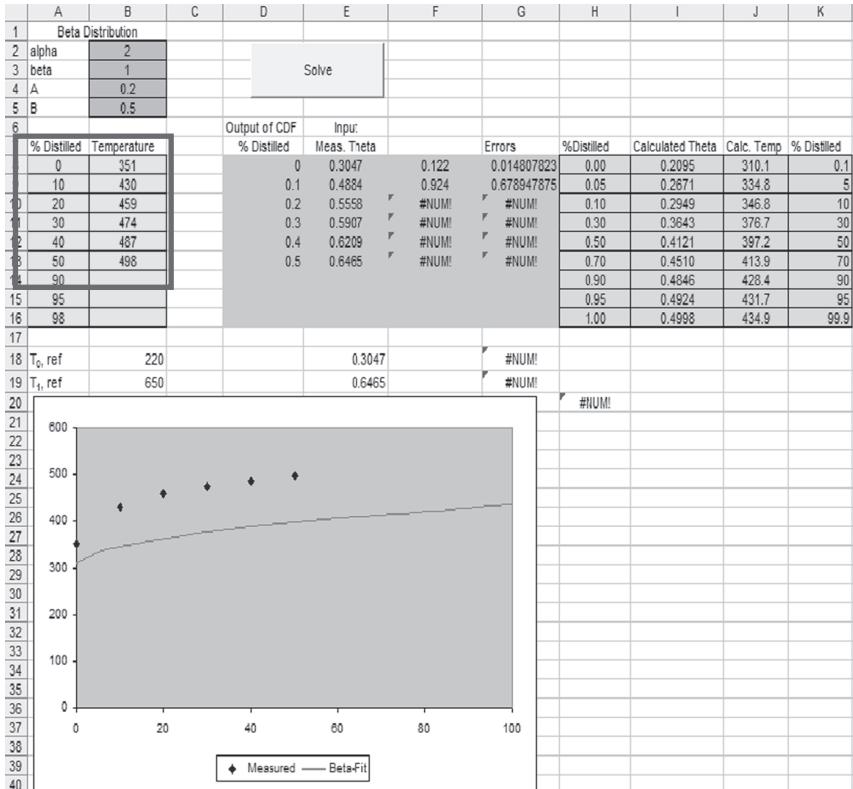


Figure 1.13 Input cells in *WS1.2 Beta.xls*.

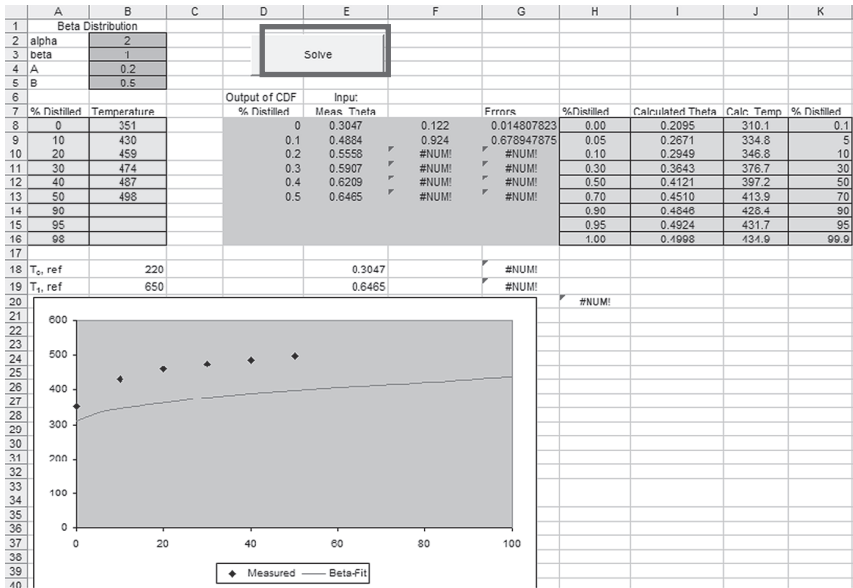


Figure 1.14 Activation button in *WS1.2 Beta.xls*.

35	Deeply hydrogenated fractions	0.9713	0.59
36	Short residues	0.9345	0.63
37	FCC feeds	0.9365	0.63
38	Coal liquids	0.9448	0.63
39	Stream cracker residue	0.881	0.7
40			
41	Selected correlation		5
42			
43			
44		FCC feeds	
45		Naphthas	
46		Straight or hydrosulfurized gas oils	
47		Deeply hydrogenated fractions	
48		Short residues	
49		FCC feeds	
50		Coal liquids	
51		Stream cracker residue	

Figure 1.17 Select oil type.

5		Vol%	Temperature (F)
6		0	310.2
7		10	341.3
8		30	369.8
9		50	387.4
10		70	406.4
11		90	433.4
12		100	480.6
13			
14	Specific gravity		0.7457
15	Refractive index @ 20 C		
16	Oxygen content (wt%)		0.00
17	Initial MeABP (F) [Enter as first guess in yellow cell]		384.93

Figure 1.18 Input distillation curve and specific gravity.

The screenshot shows the Microsoft Excel interface. The 'Tools' menu is open, and 'Goal Seek...' is highlighted. The spreadsheet data is visible in the background, matching the data in Figure 1.18.

4		A
5		Vol%
6		0
7		10
8		30
9		50
10		70
11		90
12		100
13		
14	Specific gravity	
15	Refractive index @ 20 C	
16	Oxygen content (wt%)	
17	Initial MeABP (F) [Enter as first guess in yellow cell]	
18		

Figure 1.19 Activate "goal seek" in WS1.3 MeABP Iteration.xls.

19	Trial MeABP (F)	422.00	65	70
20	Trial MeABP (R)	881.67	70	75
21	Watson-K	12.86		
22				
23	Calc. VABP (R)	847.70		
24	Calc. WABP (R)	848.19		
25	Calc. MABP (R)	845.17		
26	Calc. CABP (R)	847.21		
27				
28	Calc. MeABP (R)	846.19		
29				
30	Error (Trial MeABP - Calc. MeABP)	1258.74304		

(Use goalseek to drive green cell to 0 by c

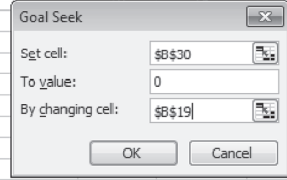


Figure 1.20 Assign tuning and objective cells.

5		Vol%	Temperature (F)
6		0	310.2
7		10	341.3
8		30	369.8
9		50	387.4
10		70	406.4
11		90	433.4
12		100	480.6
13			
14	Specific gravity		0.7457
15	Refractive index @ 20 C		
16	Oxygen content (wt%)		0.00
17	Initial MeABP (F) [Enter as first guess in yellow cell]		384.93
18			
19	Trial MeABP (F)		386.55
20	Trial MeABP (R)		846.22
21	Watson-K		12.68
22			
23	Calc. VABP (R)		847.70
24	Calc. WABP (R)		848.19
25	Calc. MABP (R)		845.19
26	Calc. CABP (R)		847.21
27			
28	Calc. MeABP (R)		846.20
29			
30	Error (Trial MeABP - Calc. MeABP)		0.00042

Figure 1.21 Iterative MeABP in WS1.3 MeABP Iteration.xls.

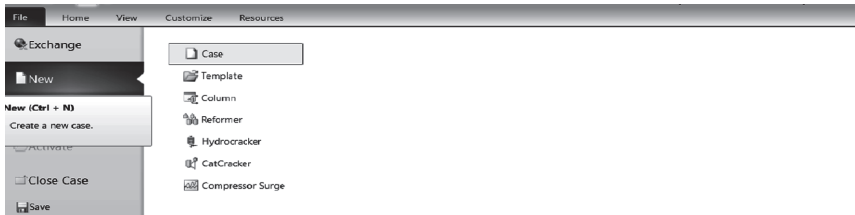


Figure 1.22 Start a new case in Aspen HYSYS Petroleum Refining.

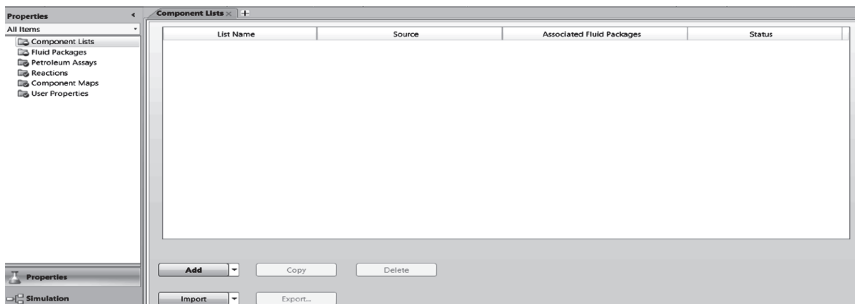


Figure 1.23 Add a new component list.

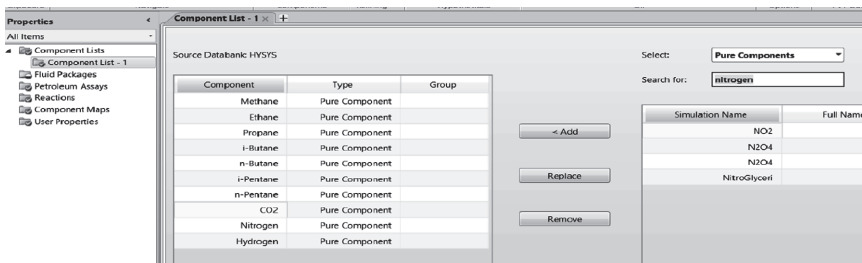


Figure 1.24 Add light components.

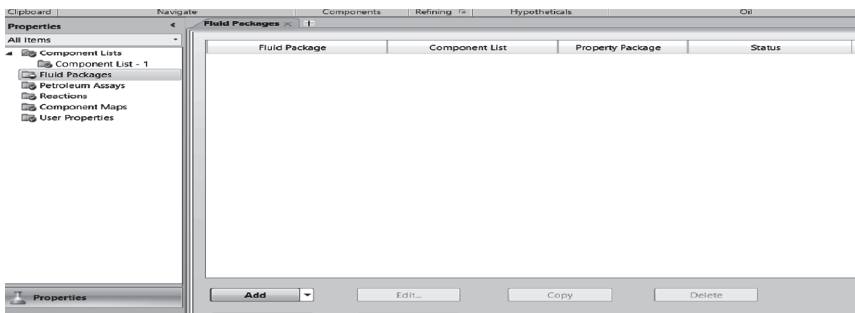


Figure 1.25 Click “add” to enter the list of thermodynamic models.

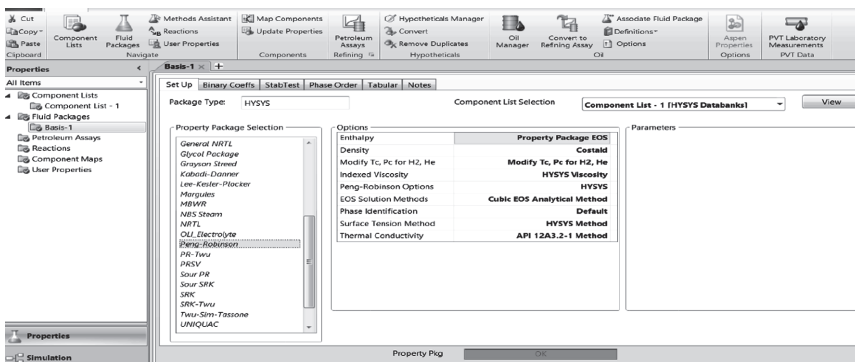


Figure 1.26 Select the Peng–Robinson thermodynamic model and click on “Oil Manager” tab.

Step 8. Check “distillation” and click “edit assay” to input the distillation curve. Refer to the data in the spreadsheet, *WS1.4 Distillation Curve and Light End Composition.xlsx*. Note that the temperature unit in Figure 1.28 is degree Fahrenheit. To change this to degree Centigrade, go to the File menu and click Options. This will open the Simulation Options window. On the Variables tab, click Units. Choose SI units and then the temperature unit becomes degree Centigrade (Figure 1.29).

Step 9. Check “bulk props” to input the bulk density and other bulk properties if available (Figure 1.30).

Step 10. Check “light ends” to input the light end composition (Figure 1.31).

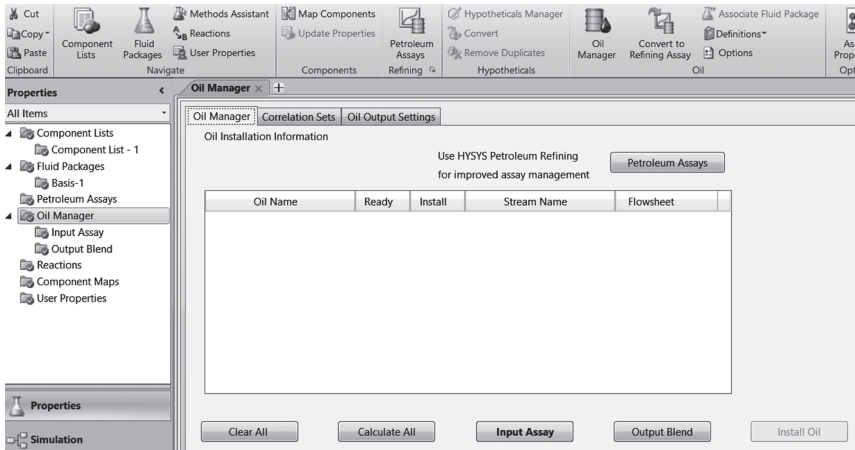


Figure 1.27 “Input Assay” to define a new assay.

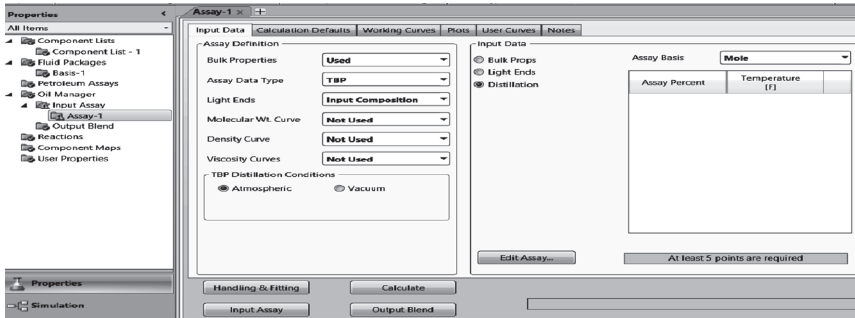


Figure 1.28 Select the data to be used to define an assay.

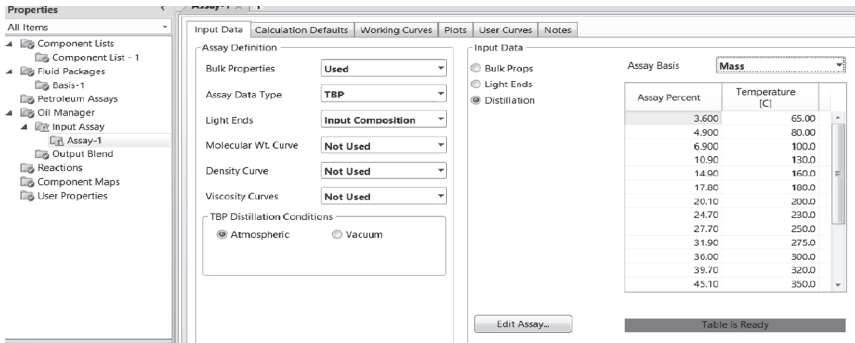


Figure 1.29 Enter the distillation curve.

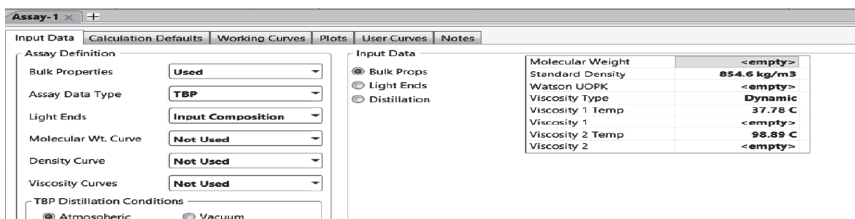


Figure 1.30 Enter the bulk density.

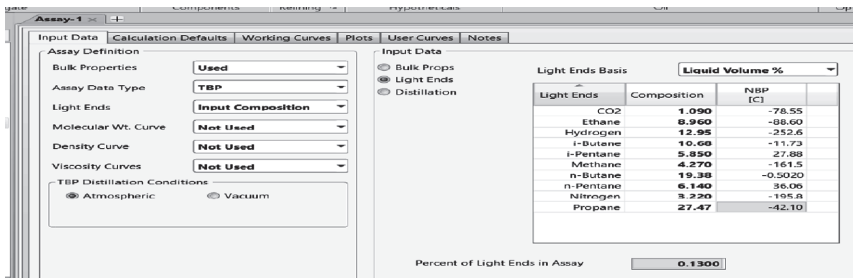


Figure 1.31 Enter the composition of light components.

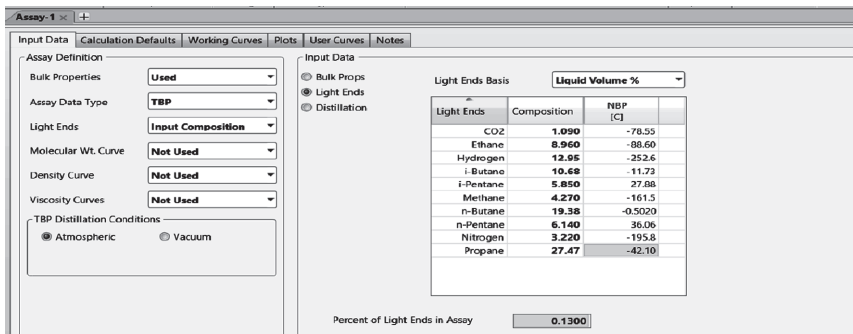


Figure 1.32 Click "calculate" for calculation and generate the pseudocomponents.

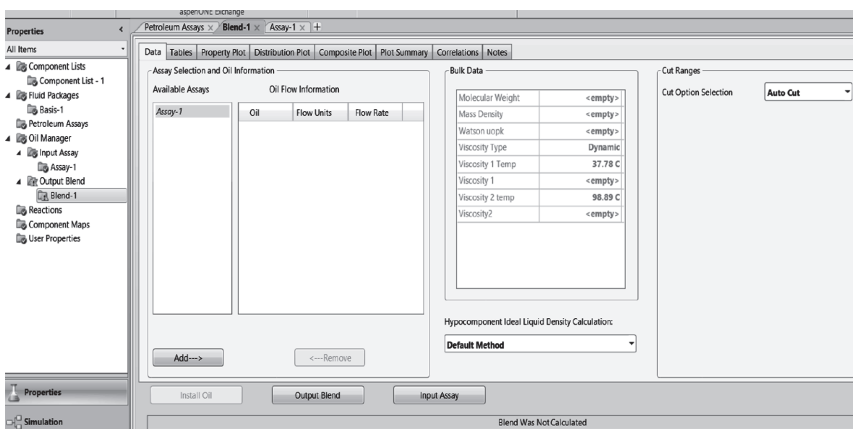


Figure 1.33 Create a new blend, Blend-1. See our previously defined assay, Assay-1.

Step 11. Click "calculate" to enable the calculations by Aspen HYSYS Petroleum Refining to generate pseudocomponents (Figure 1.32).

Step 12. Click on "Output Blend" and click "Add" to create a new blend, Blend-1 (Figure 1.33).

Step 13. Select "Assay-1" and click add to generate the corresponding pseudocomponents (Figure 1.34).

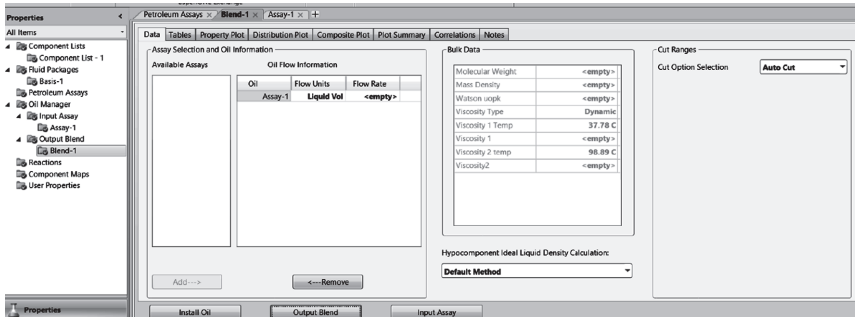


Figure 1.34 Select Assay-1 used to be cut or blended and enable the blend calculation.

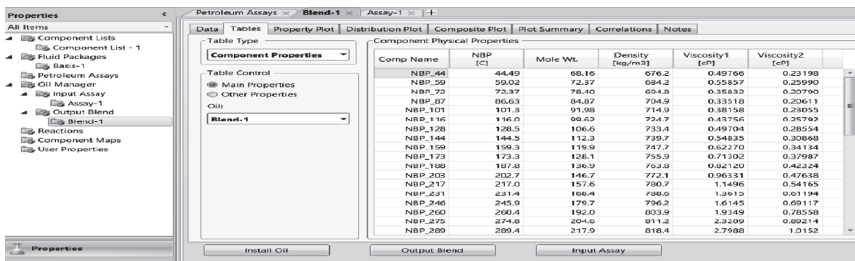


Figure 1.35 The pseudocomponents used to represent the cut or blend.

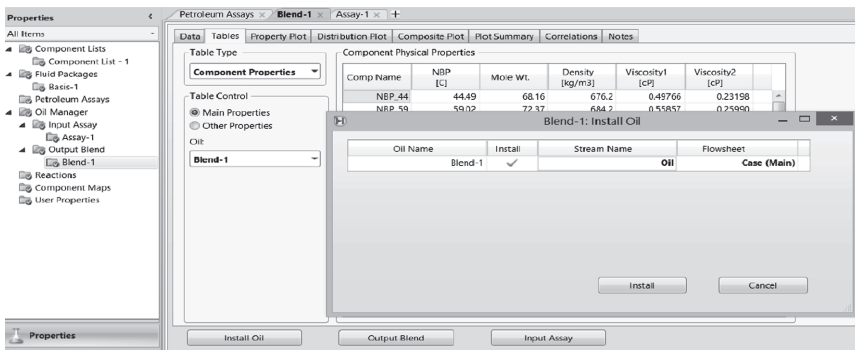


Figure 1.36 Install the cut/blend into simulation.

Step 14. Go to “Tables” tab to check the generated pseudocomponents (Figure 1.35).

Step 15. Click on “Install Oil” tab, enter “Oil” as the stream name, and click the “Install” box (Figure 1.36).

Step 16. Go to the simulation environment. The stream “Oil” represents the created oil fraction. Click on the stream to see the Composition under Worksheet. We have duplicated the oil fraction within the Oil Manager within Aspen HYSYS Petroleum Refining (Figure 1.37).

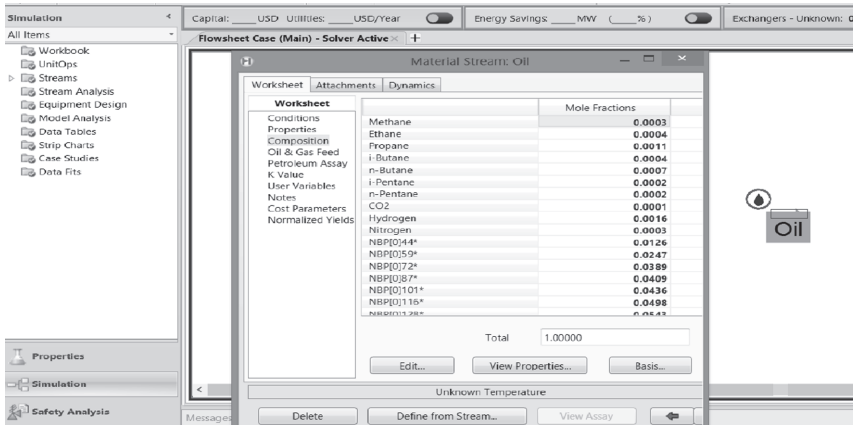


Figure 1.37 The stream in the simulation environment represents the created oil fraction.

1.7 Workshop 1.5– Represent an Oil Fraction by the New Petroleum Assay Manager in Aspen HYSYS Petroleum Refining

- Step 1.* Start a new case in Aspen HYSYS Petroleum Refining (Figure 1.38).
- Step 2.* Right-click “Petroleum Assays” and select “Add new assays” to add a new assay. Choose “Manually enter” option. For “Assay Component Selection,” choose “Assay Component Celsius to 850 °C.” Click OK (Figure 1.39).
- Step 3.* This generates the “New Assay” form of Figure 1.40a. Choose “Single Steam Properties.” Copy and paste the TBP distillation curve from

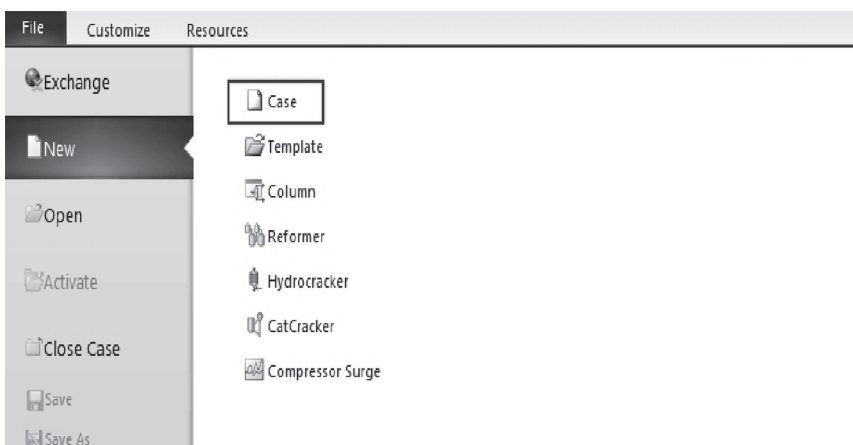


Figure 1.38 Start new case in Aspen HYSYS Petroleum Refining and save as *WS1.5 Petroleum Assay Manager.hsc*. Add the same components (C1, C2, C3, iC4, nC4, iC5, nC5, CO₂, H₂, and N₂) and fluid package (Peng–Rob) as shown in Figures 1.24 and 1.25 in *WS1.4*.

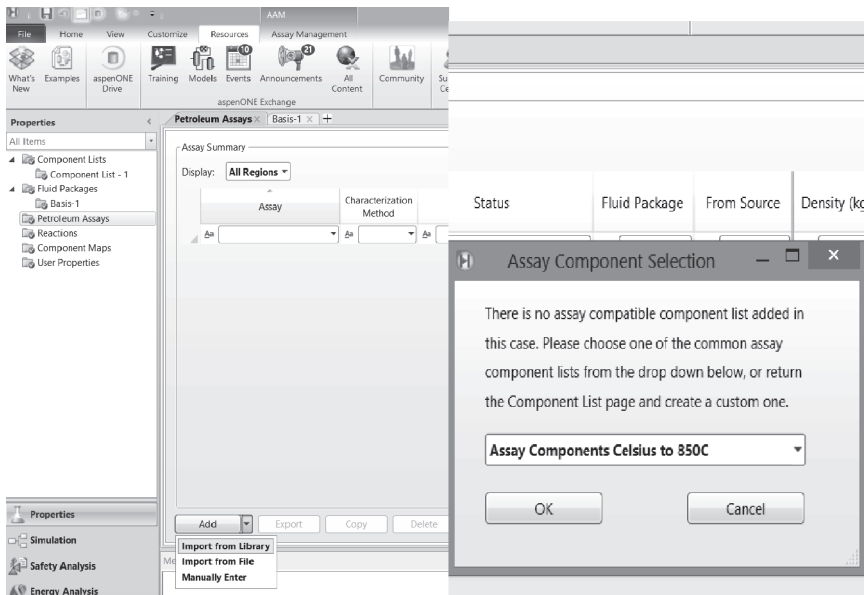
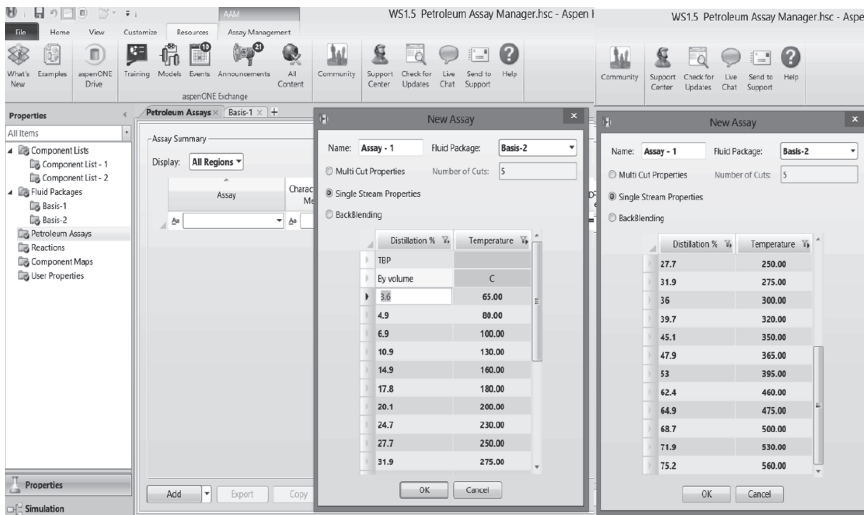
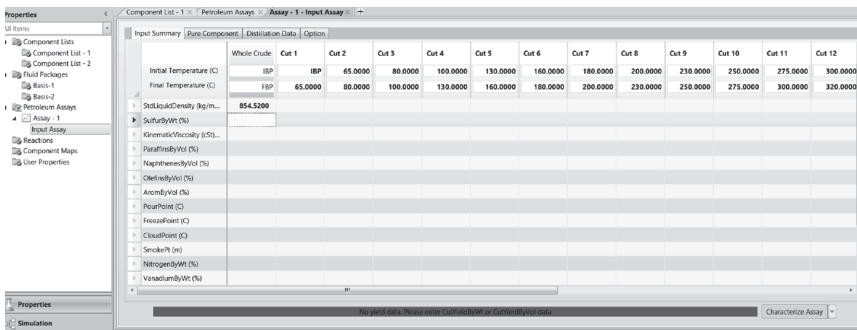


Figure 1.39 Right-click “Petroleum Assays” to add a new assay and choose “Assay Components Celsius to 850 °C” for “Assay Component Selection” and click “OK.”

- WS1.4 Distillation Curve and Light End Compositions.xls* into the New Assay form. This results in an input summary of Figure 1.40b.
- Step 4.** Input the bulk density and other bulk properties if available (Figure 1.41).
- Step 5.** In “Pure Component,” add a new cut named “LightEnd” and set the IBP as its initial temperature and final boiling point (FBP) as its final temperature. Then, input the light end compositions following the data in *WS1.4 Distillation Curve and Light End Compositions.xls* (Figure 1.42).
- Step 6.** In “Input Summary” form, click on “Characterize Assay” to enable the Aspen HYSYS Petroleum Refining to do crude characterization (Figure 1.43).
- Step 7.** After characterizing the assay, we can create plots of cut yields, distillations, crude properties, cut viscosities, and PNA (Figures 1.44 and 1.45).
- Step 8.** Click “Simulation” to enter the simulation environment (Figure 1.46).
- Step 9.** Click “Model Palette” to open the window of unit models (Figure 1.47).
- Step 10.** Click “Refining > Petroleum Feeder” to add a petroleum feed (Figure 1.48).
- Step 11.** Add a feed stream (Figure 1.49).
- Step 12.** Click the feeder and select feed assays and the product stream (Figure 1.50).



(a)



(b)

Figure 1.40 (a) Enter the TBP distillation curve into “New Assay” form. (b) The resulting input summary form.

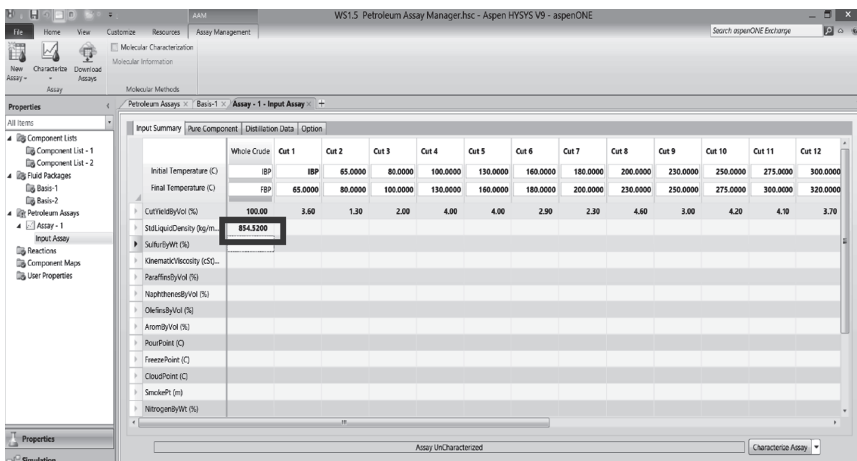


Figure 1.41 Enter the bulk density of 854.62 kg/m³.

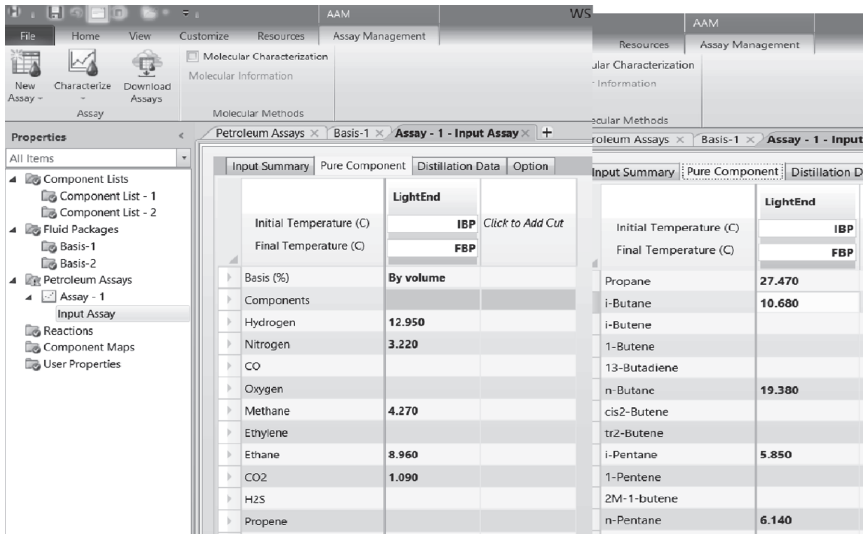


Figure 1.42 Enter the compositions of light components.

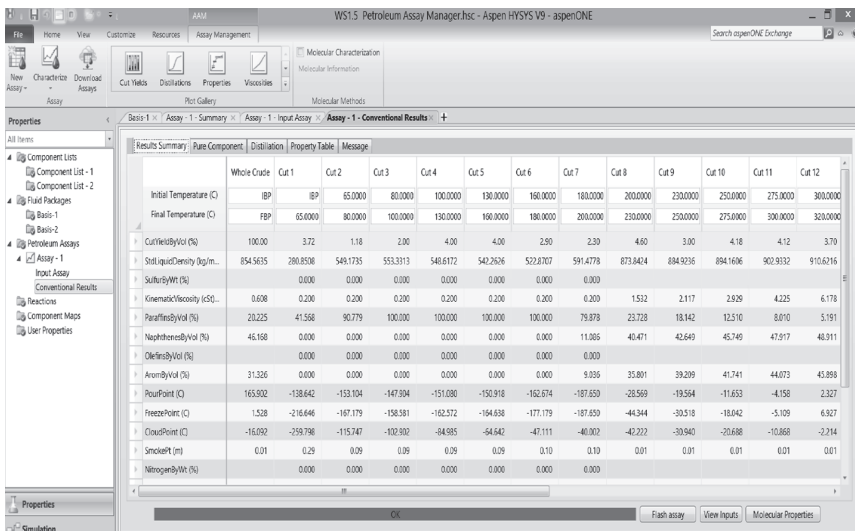


Figure 1.43 Characterize the assay.

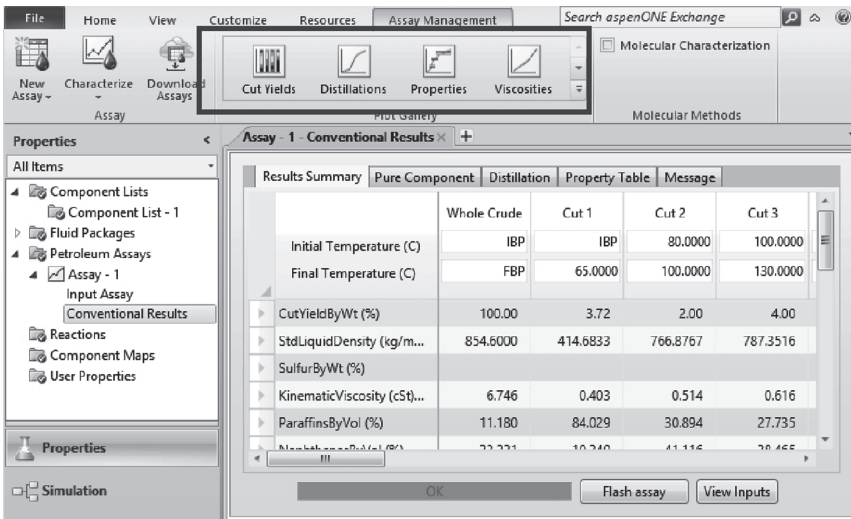


Figure 1.44 Add and edit assay data.

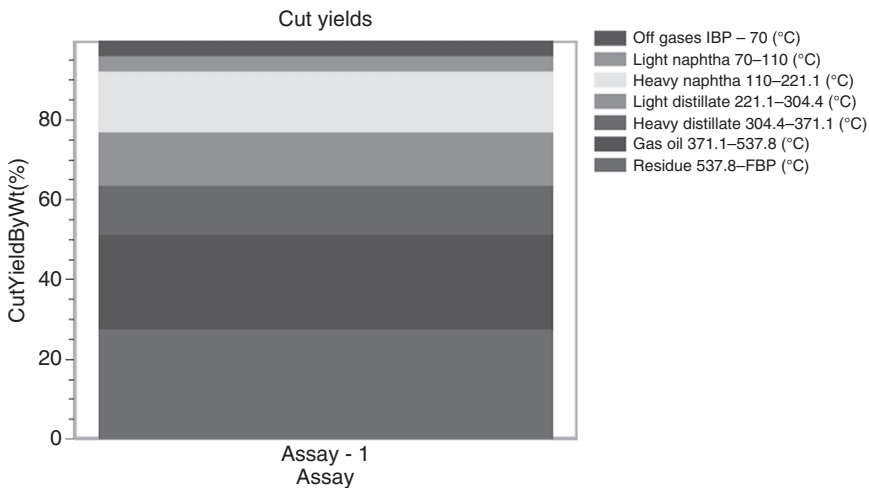


Figure 1.45 Plot of cut yields.

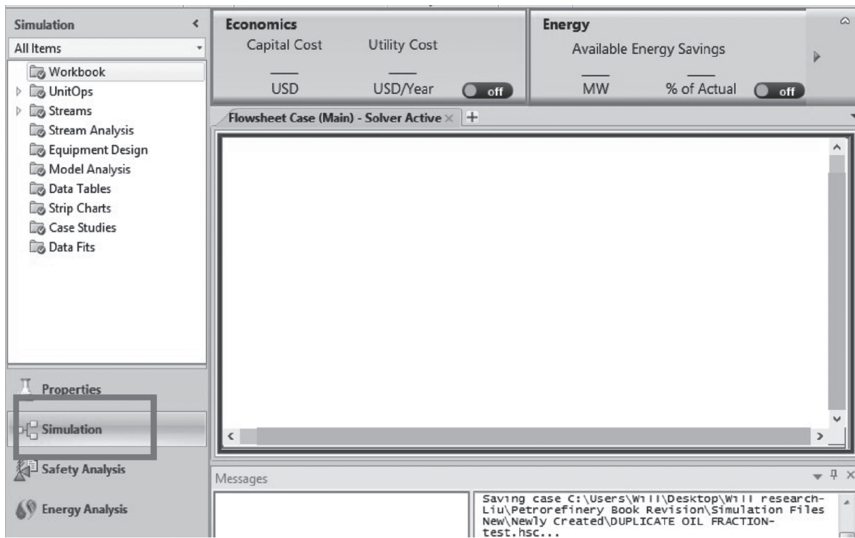


Figure 1.46 Enter the simulation environment.

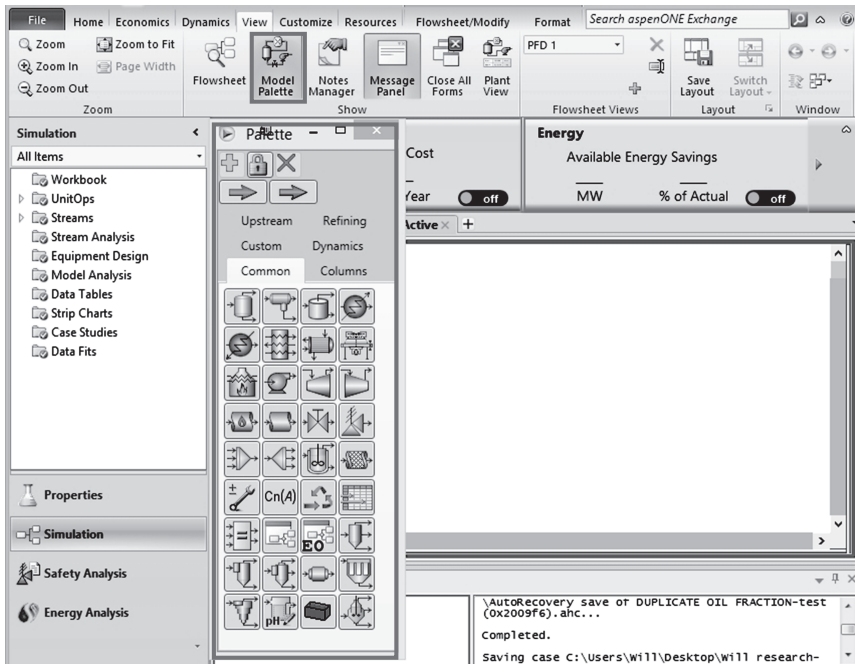


Figure 1.47 Open the window of unit models.

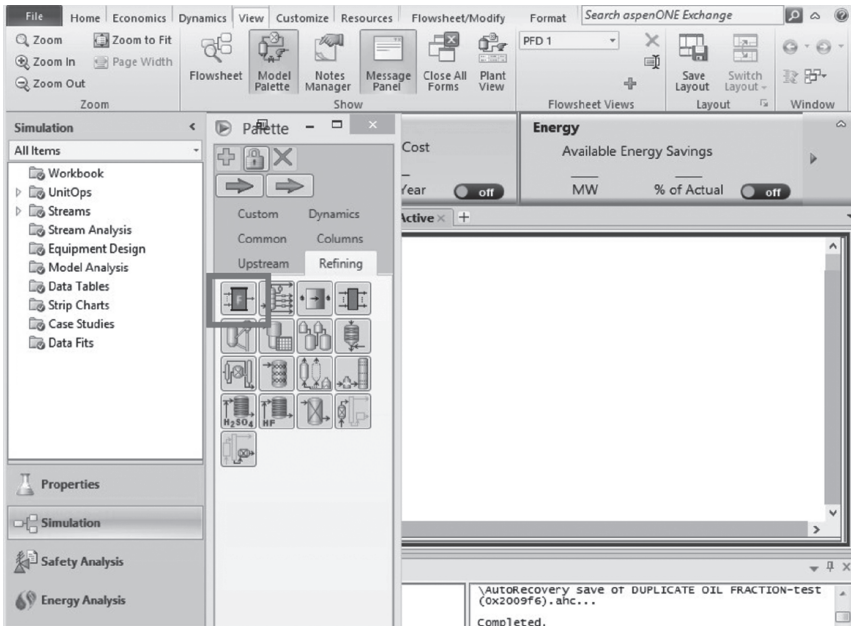


Figure 1.48 Add a petroleum feeder.



Figure 1.49 Add a feed stream.

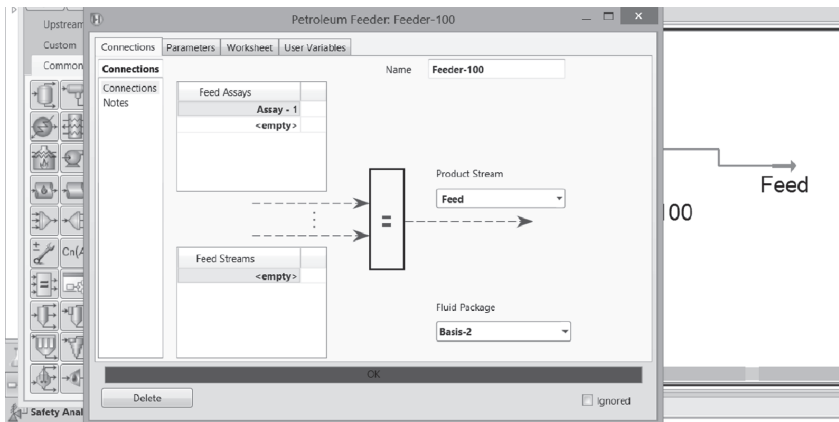


Figure 1.50 Specify feed assays in the petroleum feeder.

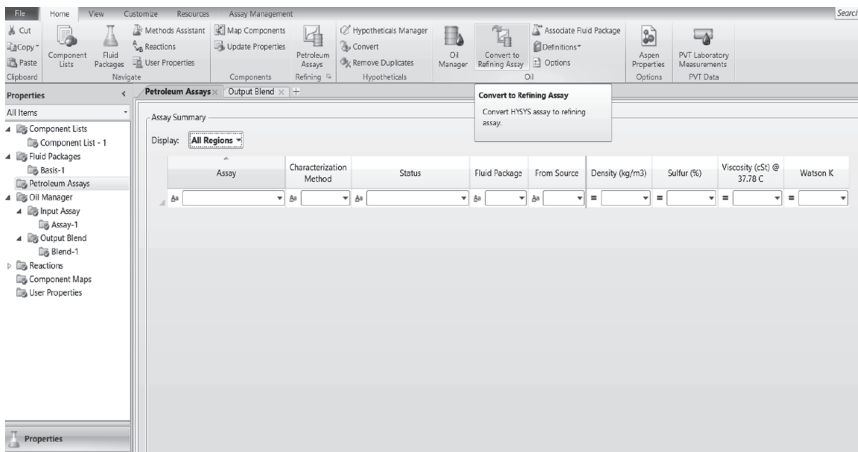


Figure 1.51 Convert the representation from oil manager to petroleum assay manager.

1.8 Workshop 1.6 – Conversion from the Oil Manager to Petroleum Assay Manager and Improvements of the Petroleum Assay Manager over the Oil Manager

We open the file, *WS1.4 Oil Manager.hsc*, and save as *WS1.6 Conversion from Oil Manager to Petroleum Assay Manager.hsc*. Figure 1.51 shows where we highlight the Petroleum Assay within the Properties Environment and then click on the button, Convert to Refinery Assay, to make the conversion.

This is given in Figure 1.52, in which we choose to use the existing fluid package and then click on Convert.

The conversion results in Figure 1.53, which is identical to the representation in the petroleum assay manager in Figure 1.42.

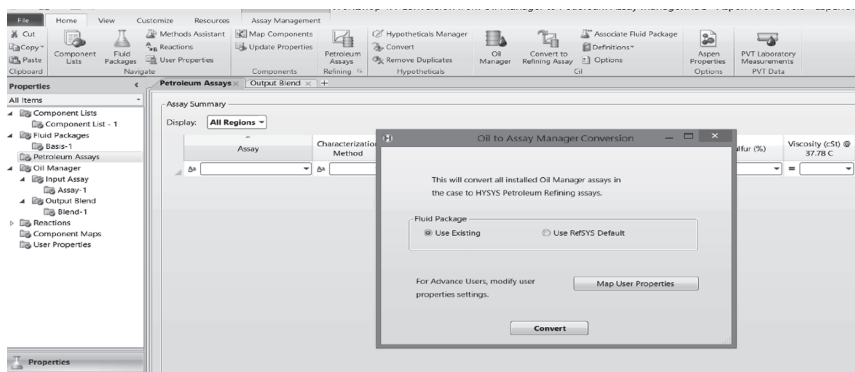


Figure 1.52 Oil to petroleum assay manager conversion.

Table 1.3 summarizes the improvements of the new petroleum assay manager over the old oil manager.

We strongly recommend the use of the petroleum assay manager to represent oil assays.

1.9 Property Requirements for Refinery Process Models

We classify the processes in modern refinery into two categories: separation units and reaction units. To develop a process model for any unit, we need to check the mass and energy balances of the flowsheet and perform calculations to describe the performance of the target unit. Therefore, the essential properties (physical and chemical) used to simulate these processes depend on the target unit, the chosen pseudocomponent scheme, and the selected kinetic model for reaction unit. Chapters 4 through 6 will represent the relevant issues for the three major reaction units in a modern refinery – FCC, catalytic reformer, and hydrocracker – and Chapter 7 covers additional refinery reaction units such as alkylation and delayed coking. While this chapter focuses primarily on the thermophysical properties required for modeling fractionation processes, the general framework for developing these properties for different kinds of pseudocomponents (i.e., those generated by kinetic lumping networks) is the same.

The previous sections in this chapter address the creation of pseudocomponents by cutting an assay curve into a set of discrete components based on boiling point ranges. We also briefly consider physical properties and process thermodynamics selection in the earlier workshops of this chapter. In this section, we discuss, in detail, the problem of how to represent these components in process modeling software. There are two major concerns in this area: physical properties of pseudocomponents and selection of a thermodynamic model that can deal with these hydrocarbon pseudocomponents in the context of refinery modeling. An accurate selection of physical properties and process thermodynamics results in a process model that can accurately account for material and energy flows in both vapor and liquid process streams.

Table 1.4 Required properties for each phase.

Phase	Required properties
Vapor	Ideal gas heat capacity (CP_{IG})
Liquid	Liquid heat capacity (CP_L), liquid density (ρ_L), latent heat of vaporization (ΔH_{VAP}), vapor pressure (P_{VAP})
Both	Molecular weight (MW)

1.10 Physical Properties

For any process simulation that involves only vapor–liquid phases, certain key physical and thermodynamic properties must be available for each phase. Table 1.4 lists these properties for all phases. We can typically obtain these properties for pure components (i.e., *n*-hexane and *n*-heptane) from widely available databases such as DIPPR [2]. Commercial process simulation software (including Aspen HYSYS) also provides access to a large set of physical and thermodynamic properties for thousands of pure components. However, using these databases requires us to identify a component by name and molecular structure first and use experimentally measured or estimated values from the same databases. Given the complexity of the crude feed, it is not possible to completely analyze the crude feed in terms of pure components. Therefore, we must be able to estimate these properties for each pseudocomponent based on certain measured descriptors.

It is important to note that the properties given in Table 1.4 are the minimal physical properties required for rigorous accounting of the material and energy flows in the process. As we discuss in the subsequent sections, process models may require additional properties (especially vapor pressure) depending on the type of thermodynamic models being considered.

1.10.1 Estimating Minimal Physical Properties for Pseudocomponents

We have shown in the previous sections that the minimal amount of information to create pseudocomponents is a distillation curve and a specific gravity or density distribution. If only the bulk density is available, we can use constant Watson *K* factor assumption to estimate the density distribution. If only a partial density distribution is available, we can use the beta function to extrapolate an incomplete distillation curve. Note that it is usually better to incorporate as much experimentally measured information about the density curve as possible when building the process model. Once the distillation and density curve are available, we can cut the curve into a set of discrete pseudocomponents, each with its own boiling point and density. We can then use these two measured properties to estimate a variety of different types of physical properties (i.e., molecular weight, critical temperature, critical pressure, and acentric factor). Using these estimated physical properties, we can derive additional estimates for minimal physical properties required for process simulation. We have also

provided a Microsoft Excel spreadsheet, *Critical_Property_Correlations.xls*, in the material that accompanies this text, which includes many of the correlations given in this section.

1.10.2 Molecular Weight

The molecular weight is the most basic information for a given pseudocomponent. Molecular weight is a required property to ensure a material balance throughout the process flowsheet. Researchers have extensively studied the trends of molecular weight for a variety of pure hydrocarbons and oil fractions. Several correlations are available to estimate the molecular weight as a function of boiling point, density, and viscosity. In general, correlations that only require the boiling point are the least accurate and correlations that require values of boiling point, density, and viscosity tend to be the most accurate. We use viscosity as a parameter in these correlations because it correlates well with molecular type – which can further refine the molecular weight estimate. In most cases, we use correlations that require the boiling point and density of a given component. Two popular correlations are the Lee–Kesler correlation [9, 10], Eq. (1.10), and the Twu correlation [11], Eqs. (1.11)–(1.13), respectively.

$$\begin{aligned} MW = & -12272.6 + 9486.4(SG) + (8.3741 - 5.99175 \cdot SG)T_b \\ & + (1 - 0.77084 \cdot SG - 0.02058 \cdot SG^2) \\ & \times \left(0.7465 - \frac{222.466}{T_b}\right) \cdot \frac{10^7}{T_b} + (1 - 0.80882 \cdot SG - 0.02226 \cdot SG^2) \\ & \times \left(0.3228 - \frac{17.335}{T_b}\right) \cdot \frac{10^{12}}{T_b^3} \end{aligned} \quad (1.10)$$

$$MW^o = \frac{T_b}{5.8 - 0.0052T_b} \quad (1.11)$$

$$SG^o = 0.843593 - 0.128624\alpha - 3.36159\alpha^3 - 13749.5\alpha^{12} \quad (1.12)$$

$$\begin{aligned} T_c^o = & T_b(0.533272 + 0.343838 \times 10^{-3} \times T_b + 2.52617 \times 10^{-7} \times T_b^2 \\ & - 1.654881 \times 10^{-10} \times T_b^3 + 4.60773 \times 10^{-24} \times T_b^{-13})^{-1} \end{aligned} \quad (1.13)$$

$$\alpha = 1 - \frac{T_b}{T_c^o} \quad (1.14)$$

$$\ln(MW) = \ln(MW^o) \left[\frac{(1 + 2f_M)}{(1 - 2f_M)^2} \right] \quad (1.15)$$

$$f_M = \Delta SG_M \left[\chi + \left(-0.0175691 + \frac{0.143979}{T_b^{0.5}} \right) \right] \Delta SG_M \quad (1.16)$$

$$\chi = \left| 0.012342 - \frac{0.244515}{T_b^{0.5}} \right| \quad (1.17)$$

$$\Delta SG_M = \exp[5(SG^o - SG)] - 1 \quad (1.18)$$

Riazi [4] listed several other correlations such as Cavett and Goosens for molecular weight, but they generally do not have significant advantage over the Lee–Kesler or Twu correlations. The Lee–Kesler correlation was developed by

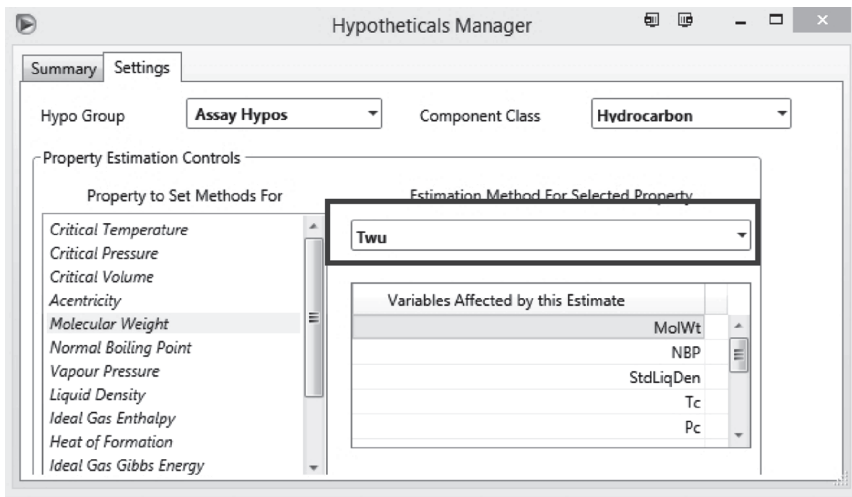


Figure 1.55 Modify the molecular weight correlation in Aspen HYSYS Hypotheticals Manager.

correlating light oil fractions ($<850^{\circ}\text{F}$ or 454°C) from a variety of sources. As a result, the Lee–Kesler correlation tends to be less accurate for pseudocomponents with high boiling point temperatures. The Twu correlation includes a significant number of data points to account for heavier components. Aspen HYSYS uses the Twu correlation to calculate the molecular weight. Figure 1.55 shows how to select the molecular weight correlation for a particular blend (shown in earlier workshops) in Aspen HYSYS Hypotheticals Manager.

1.10.3 Critical Properties

Many properties that are required for rigorous accounting of material and energy flows (Table 1.4) in process models are not well defined for pseudocomponents. Fortunately, researchers have found that these required properties correlate well with critical temperature (T_c), critical pressure (P_c), and acentric factor (ω) for different types of hydrocarbons from many sources. Therefore, when we use pseudocomponents of any kind, we must also estimate these critical properties. Just as with molecular weight, many critical property estimation methods are available in the literature. These correlations differ on the basis of the parameters required and underlying data used to create the correlation. We note that as the components get heavier and boil at higher temperatures, the associated change in critical pressure tends to diminish. Hence, correlations for critical pressure tend to be logarithmic formulas. A modeling consequence is that particularly accurate measures of these critical pressures are not required for good modeling results. In addition, most refinery process conditions do not approach the critical properties of these pseudocomponents.

Lee–Kesler [9, 10] and Twu [11] have also produced correlations for critical properties. In our work, we have used the Lee–Kesler correlations extensively. Equations (1.19) and (1.20) give the correlations for critical temperature (T_c) and critical pressure (P_c) using the Lee–Kesler correlations. We recommend using

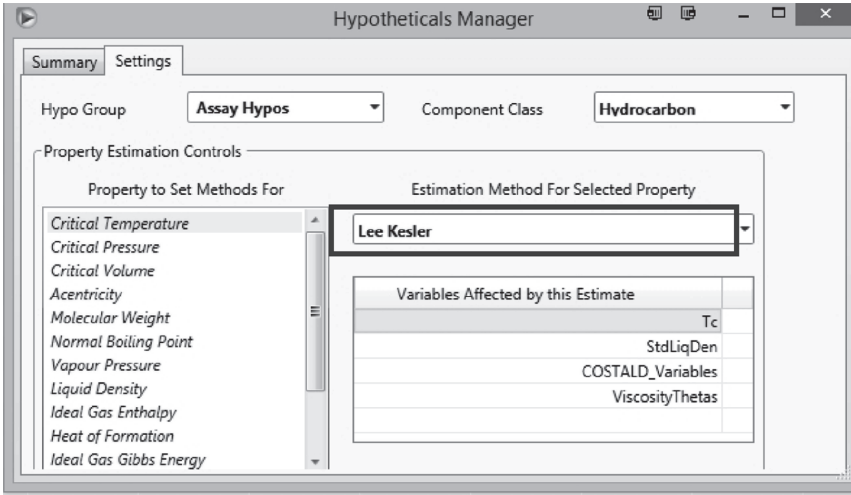


Figure 1.56 Modify T_c correlation in Aspen HYSYS Hypotheticals Manager.

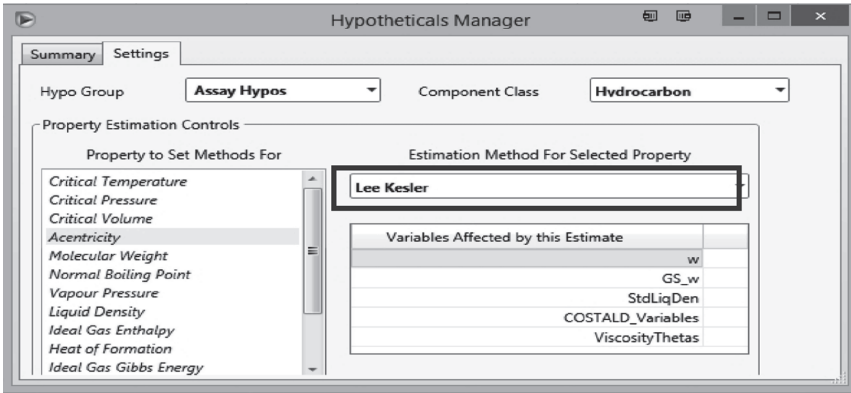


Figure 1.57 Modify acentric factor correlation in Aspen HYSYS Hypotheticals Manager.

these correlations for all boiling point ranges as the differences that arise from using other correlations are often minor. Figures 1.56 and 1.57 show how we can change the correlation for each blend in Aspen HYSYS Hypotheticals Manager.

$$T_c = 189.8 + 450.6SG + (0.4244 + 0.1174SG)T_b + (0.1441 - 1.0069SG)10^5/T_b \quad (1.19)$$

$$P_c = 5.689 - \frac{0.0566}{SG} - \left(0.43639 + \frac{4.1216}{SG} + \frac{0.21343}{SG^2}\right) \times 10^{-3}T_b + \left(0.47579 + \frac{1.182}{SG} + \frac{0.15302}{SG^2}\right) \times 10^{-6}T_b^2 - \left(2.4505 + \frac{9.9099}{SG^2}\right) \times 10^{-10}T_b^3 \quad (1.20)$$

A related property is the acentric factor. The acentric factor accounts for the size and shape of various kinds of molecules. Simple molecules have an acentric factor close to 0, whereas large or complex hydrocarbon molecules may have values approaching 0.5–0.6 [6]. The acentric factor is not measured but defined as an explicit function of the ratio of vapor pressure at the normal boiling point to the measured or estimated critical pressure. We show the definition of the acentric factor in Eq. (1.21).

$$\omega = -\log_{10}(P_r^{\text{VAP}}) - 1.0 \quad (1.21)$$

where P_r^{VAP} represents the reduced vapor pressure, that is, the pseudocomponent vapor pressure divided by its critical pressure, when the reduced temperature, T_r , that is, the temperature divided by the critical temperature, is equal to 0.7.

Given the small range of values for the acentric factor, most correlations can provide useful results. The accuracy of the acentric correlation depends largely on the accuracy of the critical temperature and pressure correlations. However, even large relative errors do not result in significant deviation of derived properties such as ideal gas heat capacity. We again choose the Lee–Kesler [9, 10] correlation for the acentric factor. This correlation, given by Eq. (1.22), relies on extensive vapor pressure data collected by Lee and Kesler for the critical temperature and pressure correlations. The correlation is technically limited to the reduced boiling point temperature (T_{br}) of less than 0.8 but has been successfully used at high T_{br} values. Figure 1.57 shows how we can modify the acentric factor estimation method for oil blends in Aspen HYSYS Hypotheticals Manager.

$$\omega = \frac{-\ln(P_c/1.01325) - 5.92714 + \frac{6.09648}{T_{\text{br}}} + 1.28862 \ln(T_{\text{br}}) - 0.169347 T_{\text{br}}^6}{15.2518 - \frac{15.6875}{T_{\text{br}}} - 13.4721 \ln(T_{\text{br}}) + 0.43577 T_{\text{br}}^6} \quad (1.22)$$

In this equation, T_{br} represents the reduced boiling point, that is, the normal boiling point divided by the critical temperature T_c .

1.10.4 Liquid Density

The liquid density of hydrocarbons is essential for modeling purposes to convert molar and mass flows into volumetric flows. Many processes in the refinery operate on the basis of volumetric flow. In addition, the density of the products is an important constraint while marketing the refinery's products for sale. In the context of process modeling, liquid density is also a property parameter that must be correlated as many of the equation-of-state (EOS) thermodynamic models cannot accurately predict liquid densities. Even when a given process modeling software uses an EOS approach for refinery modeling, liquid density is often calculated independently to ensure accurate results. Figure 1.58 shows how Aspen HYSYS calculates the liquid density independently even when we use an EOS (in this case, Peng–Robinson) as the thermodynamic model.

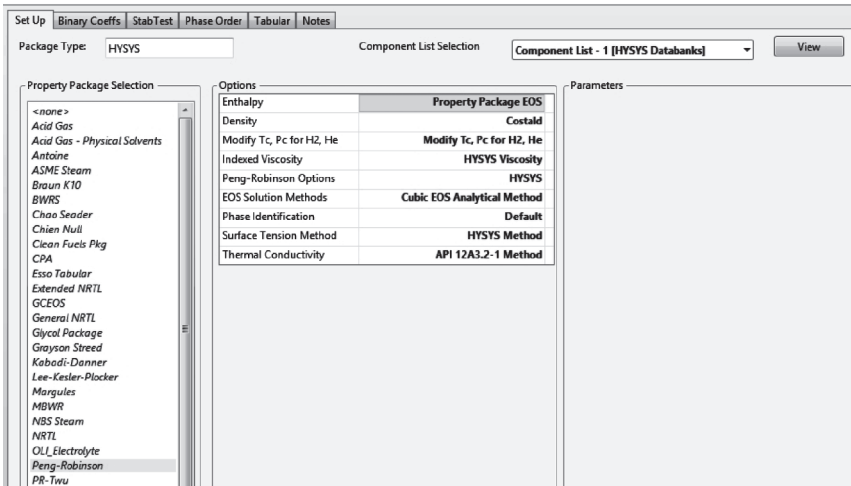


Figure 1.58 Options for Peng–Robinson equation of state in Aspen HYSYS.

Several correlations are available in the literature for liquid mass density or liquid molar volume as functions of various critical properties. It is possible to convert from liquid mass density to liquid molar volume using the molecular weight of the component in question. This also means that errors in the molecular weight or critical property predictions can introduce additional error in the liquid density or molar volume correlations. Popular correlations for liquid density include Yen–Woods [12], Gunn–Yamada [13], and Lee–Kesler [9, 10]. An accurate correlation (when the reduced temperature is less than 1) of liquid density is the Spencer–Danner (modified Rackett) method [14] with COSTALD (Corresponding States Liquid Density) [15] correction for pressure. Equation (1.23) gives the standard Spencer–Danner equation. This equation actually predicts the molar volume at saturated liquid conditions. We can convert this molar volume into liquid density using the molecular weight.

$$V^{\text{SAT}} = \left(\frac{RT_C}{P_C} \right) Z_{\text{RA}}^n \quad \text{with } n = 1.0 + (1.0 - T_r)^{2/7} \quad (1.23)$$

$$Z_{\text{RA}} = 0.29056 - 0.08775\omega \quad (1.24)$$

Z_{RA} is a special parameter to account for the critical compressibility of the component. Tables of Z_{RA} for many pure components are part of the pure component databases in Aspen HYSYS. We may estimate Z_{RA} for pseudocomponents from Eq. (1.24) as a function of the correlated acentric factor. The liquid density from Spencer–Danner equation is a function of temperature only. Refinery processing conditions can be severe enough where the liquid density is also a function of pressure. To correct the liquid density for high pressure, we can introduce the COSTALD correction given by Eq. (1.25). This equation requires the liquid density, ρ_{p^0} , at a certain reference pressure, P^0 , obtained from

Eq. (1.25) and predicts the density, ρ_p , at an elevated pressure, P , as a function of two parameters, C and B .

$$\rho_p = \rho_{p^o} \left[1 - C \ln \left(\frac{B + P}{B + P^o} \right) \right]^{-1} \quad (1.25)$$

$$e = \exp(4.79594 + 0.250047\omega + 1.14188\omega^2) \quad (1.26)$$

$$B = P_c(-1 - 9.0702(1.0 - T_r)^{\frac{1}{3}} + 62.45326(1.0 - T_r)^{\frac{2}{3}} - 135.1102(1.0 - T_r) + e(1.0 - T_r)^{\frac{4}{3}}) \quad (1.27)$$

$$C = 0.0861488 + 0.0344483\omega \quad (1.28)$$

The COSTALD correlation is quite accurate even at high reduced temperatures and pressures. Predicted liquid densities generally agree with measured values within 1–2%, provided the errors in the critical property predictions are low. A potential problem can occur if the reduced temperature is greater than 1. There can be discontinuity from the Spencer–Danner equation in the density prediction, which may cause some process models to fail. However, at a reduced temperature greater than 1, the EOS becomes more accurate and can be used directly. Aspen HYSYS includes a smoothing approach (using the Chueh and Prausnitz correlation [16]) to ensure a smooth transition from the COSTALD densities to EOS-based densities.

1.10.5 Ideal Gas Heat Capacity

The last property that is often directly correlated is the ideal gas heat capacity of pseudocomponents. The ideal gas heat capacity represents the vapor heat capacity of the pseudocomponent at a given standard condition. The standard conditions typically refer to 25 °C and 1 atm or 77 °F and 14.696 psia. It is well known that the heat capacity of hydrocarbons can be modeled with a simple polynomial expression as a function of temperature. Lee and Kesler [9, 10] presented a popular correlation, Eq. (1.29) to Eq. (1.36), where M is molecular weight, T in Kelvin, and K_w is Watson K factor. These parameters may be estimated from other correlations, including Lee–Kesler equation for MW in Section 1.10.3, Eq. (1.10). The heat capacities of hydrocarbons do not vary significantly over a wide range of temperatures, so very accurate heat capacities are not necessary for good modeling results. We present this correlation in Eq. (1.29). Figure 1.59 shows how we can modify the ideal gas heat capacity estimation method for oil blends in Aspen HYSYS Hypotheticals Manager.

$$CP_{ig} = MW[A_0 + A_1 T + A_2 T^2 - C(B_0 + B_1 T + B_2 T^2)] \quad (1.29)$$

$$A_0 = -1.41779 + 0.11828K_w \quad (1.30)$$

$$A_1 = -(6.99724 - 8.69326K_w + 0.27715K_w^2) \times 10^{-4} \quad (1.31)$$

$$A_2 = -2.2582 \times 10^{-6} \quad (1.32)$$

$$B_0 = 1.09223 - 2.48245\omega \quad (1.33)$$

$$B_1 = -(3.434 - 7.14\omega) \times 10^{-3} \quad (1.34)$$

$$B_2 = -(7.2661 - 9.2561\omega) \times 10^{-7} \quad (1.35)$$

$$C = \left[\frac{(12.8 - K_w) \times (10 - K_w)}{10\omega} \right]^2 \quad (1.36)$$

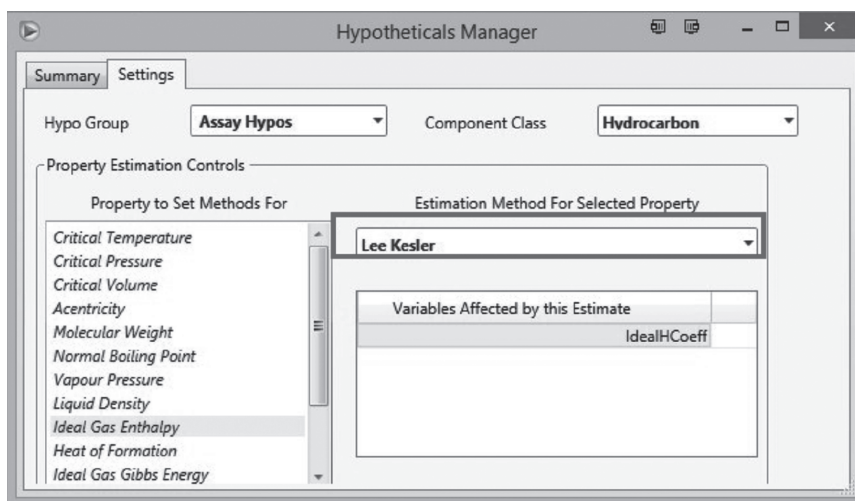


Figure 1.59 Modify ideal gas heat capacity correlation in Aspen HYSYS Hypotheticals Manager.

1.10.6 Other Derived Physical Properties

Once we have obtained the boiling point, density or specific gravity, molecular weight, and critical properties of a particular pseudocomponent, we can also generate estimates for other required properties for process simulation provided in Table 1.4. The accuracy of these predictions is largely a function of the accuracy of the molecular weight and critical property predictions. In addition, depending on the thermodynamic method chosen, we may not require any correlations for certain properties. For example, if we choose an EOS, we do not require any additional correlations for the vapor pressure (P_{VAP}) or heat of vaporization (ΔH_{VAP}), as these values will be calculated directly by the EOS. We discuss such features of the EOS in the following section. In this section, we present correlations for all required properties so that model developers are aware of the model limitations and additional data requirements when we do not use an EOS for modeling process thermodynamics.

The liquid heat capacity of pseudocomponents in refinery modeling is largely constant. Walas [6] noted that as the boiling point and density of the pseudocomponent increase, the heat capacity of hydrocarbons tends to approach a value of 1.8–2.2 kJ/kg K near the normal boiling point. Consequently, rough estimates of heat liquid capacities do not affect model results significantly. Two correlations are available for liquid heat capacities of hydrocarbons that are in general use. Equation (1.37) is a correlation by Kesler and Lee [9, 10] and Eq. (1.41) is a correlation recommended by API. Either correlation may be used with equally acceptable results. We generally do not encounter these temperature limits prescribed for both of these correlations. We also note that these correlations are weak functions of temperature. Process modeling software programs have a variety of models to estimate liquid heat capacity, but these methods are only marginally better when compared to the simple correlations given here.

When $145 \text{ K} < T < 0.8T_c$

$$CP_L = a(b + cT) \quad (1.37)$$

$$a = 1.4651 + 0.2302K_w \quad (1.38)$$

$$b = 0.306469 - 0.16734SG \quad (1.39)$$

$$c = 0.001467 - 0.000551SG \quad (1.40)$$

When $T_r < 0.85$

$$CP_L = A_1 + A_2T + A_3T^2 \quad (1.41)$$

$$A_1 = -4.90383 + (0.099319 + 0.104281SG)K_w + \left(\frac{4.81407 - 0.194833K_w}{SG} \right) \quad (1.42)$$

$$A_2 = (7.53624 + 6.214610K_w) \times \left(1.12172 - \frac{0.27634}{SG} \right) \times 10^{-4} \quad (1.43)$$

$$A_3 = -(1.35652 + 1.11863K_w) \times \left(2.9027 - \frac{0.70958}{SG} \right) \times 10^{-7} \quad (1.44)$$

Another property related to the heat capacity is the heat of vaporization of pseudocomponent as a liquid. The heat of vaporization represents the heat required to vaporize a given mass (or volume) of liquid into vapor. Similar to heat capacities, there are several correlations to calculate the heat of vaporization in the literature. We present two popular correlations here. Equation (1.45) is the Riedel correlation [17] and Eq. (1.46) is the Chen and Vetter correlation [17]. We note that both correlations rely on critical temperatures and pressure and give the heat of vaporization at the normal boiling point. We can obtain the heat of vaporization at a different temperature by using the Watson relation [1] in Eq. (1.47). Either of the correlations can provide very good results for hydrocarbons (<2% average relative deviation, ARD). We recommend the use of either correlation if the process modeling software does not already include a correlation. In addition to these correlations, Aspen HYSYS offers a more advanced proprietary correlation using two reference state liquids.

$$\Delta H_{\text{NBP}}^{\text{VAP}} = 1.093RT_c T_{\text{br}} \frac{\ln P_c - 1.013}{0.93 - T_{\text{br}}} \quad (1.45)$$

$$\Delta H_{\text{NBP}}^{\text{VAP}} = RT_c T_{\text{br}} \frac{3.978T_{\text{br}} - 3.958 + 1.555 \ln P_c}{1.07 - T_{\text{br}}} \quad (1.46)$$

$$\Delta H^{\text{VAP}} = \Delta H_{\text{NBP}}^{\text{VAP}} \left(\frac{1 - T_r}{1 - T_{\text{br}}} \right)^{0.38} \quad (1.47)$$

The vapor pressure of pseudocomponents is also an important property when an EOS is not used. All other approaches to process thermodynamics require some form of vapor pressure correlation. The vapor pressure for pure hydrocarbons has been extensively tabulated in many component databases such as DIPPR (Design Institute for Physical Property Research, American Institute of Chemical Engineers) and significant libraries are available in modern process modeling software. Several correlations for the vapor pressure of pseudocomponents are available in the literature. It is important to recall that the vapor pressure and

heat vaporization are related through the Clausius–Clapeyron equation (Eq. 1.48) [17]. This relationship imposes a constraint if we wish the model to be thermodynamically consistent. In general, most of the popular correlations for vapor pressure such as the Lee–Kesler [9, 10] agree well with heat of vaporization correlations and maintain thermodynamic consistency. We present the Lee–Kesler vapor pressure correlation in Eq. (1.49).

$$\frac{d \ln P}{dT} = \frac{\Delta H_{\text{VAP}}}{RT^2} \quad (1.48)$$

$$\ln P_r^{\text{VAP}} = 5.92714 - \frac{6.096648}{T_r} - 1.28862 \ln T_r + 0.169347 T_r^6 + \omega \left(15.2518 - \frac{15.6875}{T_r} - 13.4721 \ln T_r + 0.43577 T_r^6 \right) \quad (1.49)$$

The Lee–Kesler correlation for vapor pressure is quite accurate for low-to-medium boiling pseudocomponents. For very light components, we recommend using pure component properties directly. In the case of heavy components, Ambrose [17] has presented an additional term for the Lee–Kesler correlation. In practice, however, the additional term is not necessary for refinery modeling purposes.

1.11 Process Thermodynamics

After we have fully characterized the pseudocomponents and any true components in the process model, we must choose a thermodynamic model. The thermodynamic model here refers to a framework that allows us to describe whether a particular mixture of components forms one phase or two phases, the distribution of components within these phases, and material and energy flows of these phases given a set of process conditions. Process thermodynamics also set material and energy transfer limits on various fractionation and reaction units in the model and in the actual plant itself.

Modern refineries deal with a multitude of complex systems that may require different thermodynamic models for each refinery plant and its associated process model. For example, we cannot model the sour gas units that deal with acid gases and water with the same thermodynamic model that we use for the crude fractionation system. In fact, reasonable thermodynamic models form the heart of any process model. Chen and Mathias [7] have documented a variety of thermodynamic models available for frequently encountered chemical and physical systems. Agarwal *et al.* [18] presented a detailed account about the pitfalls of choosing a poor thermodynamic system for process models and the undesired consequences of using these poor models to modify plant operations. Process model developers and users must be aware of the underlying thermodynamics and its limitations.

Given that the field of thermodynamic models is vast, we choose to focus on thermodynamic models that deal with hydrocarbon–hydrocarbon interactions only and can model many units in the refinery quite accurately. The only complication (aside from the choice of an appropriate thermodynamic model) is the

presence of large amounts of water in the form of steam in various fractionation and reaction units. In most cases, we can simply deal with the hydrocarbon and water phases as immiscible. This is known as *the free-water approach*. Kaes [1] discussed this approach extensively and it is a common approach in many process simulators. Some software may include *a dirty-water approach*. This approach uses correlations to model the solubility of water in the hydrocarbon and the solubility of light acid gases in water. For the purposes of refinery reaction and fractionation modeling in this text, both approaches have negligible effects on the overall process model. We give the general statement of vapor–liquid equilibrium for any thermodynamic model in Eq. (1.50).

$$y_i \varphi_i^V P = x_i \varphi_i^L P \quad (1.50)$$

where y_i refers to vapor phase molar composition of component i , φ_i^V refers to the vapor phase fugacity coefficient of component i , P is overall pressure, x_i is the liquid phase molar composition of component i , and φ_i^L refers to the liquid phase fugacity coefficient of component i .

For refinery fractionation modeling, several simplifications are possible. Each one of these simplifications represents a different thermodynamic approach. We list major approaches, required pseudocomponent properties, and our recommendation for use in Table 1.5. We discuss each of these approaches and their requirements in subsequent sections.

Table 1.5 Comparison of various thermodynamic approaches.

Approach	Required physical properties	Recommended
Simple	Molecular weight (MW) Ideal gas heat capacity (CP_{IG}) Vapor pressure (P_{VAP}) Heat of vaporization (ΔH_{VAP}) Liquid heat capacity (CP_L) Liquid density (ρ_L)	No
Mixed or activity coefficient	Molecular weight (MW) Ideal gas heat capacity (CP_{IG}) Vapor pressure (P_{VAP}) Heat of vaporization (ΔH_{VAP}) Liquid heat capacity (CP_L) Liquid density (ρ_L) Solubility parameter (δ)	Yes, however, best with heavy components that the equation-of-state (EOS) approach cannot deal with
Equation of state	Molecular weight (MW) Critical temperature (T_c) Critical pressure (P_c) Acentric factor (ω) Ideal gas heat capacity (CP_{IG}) Liquid density (ρ_L) Interaction parameter (k_{ij})	Yes, with adequate corrections of liquid density

1.11.1 Process Thermodynamics

The simple approach is the most basic and least rigorous thermodynamic approach. In the simple approach or Raoult's law approach, we assume that vapor phase and liquid phase are ideal. In this case, we may write the general statement of equilibrium equation (1.50), as Eq. (1.51), where y_i is the vapor phase molar composition of component i , P is the pressure, x_i is the liquid phase molar composition, and $P^{\text{SAT}}(T)$ is the vapor pressure of component i as a function of temperature only. These properties are routinely available for pure components and we have extensively discussed how to obtain the required properties from pseudocomponents.

$$y_i P = x_i P^{\text{SAT}}(T) \quad (1.51)$$

A variation of this equation is to rearrange the equation to obtain the equilibrium distribution ratio, y_i/x_i as shown in Eq. (1.52). This distribution ratio is also known as the K -value for component i . Numerous correlations for K -values exist for a variety of pure components and pseudocomponents. The Braun-K10 (BK-10) correlation is a popular correlation of this type [6].

$$K_i = \frac{y_i}{x_i} = \frac{P^{\text{SAT}}(T)}{P} = f(T) \quad (1.52)$$

Once we obtain a K -value at a given temperature and pressure, we can perform mass and energy balances that include isothermal, isobaric, and isenthalpic flashes. We can also use the ideal gas heat capacity of the vapor phase, heat of vaporization, and heat of capacity of the liquid to represent the enthalpies of relevant vapor and liquid streams.

Most process simulators include these types of correlations, but they are largely of historical interest or used to maintain compatibility with old models. We do not recommend using simple methods, as they cannot adequately quantify the transition from vapor to liquid phases beyond the original correlation. In addition, these correlations tend to be thermodynamically poor (do not consider any interactions between components and thermodynamically inconsistent at higher pressures). We cannot integrate models using these correlations into new models that use an EOS or activity coefficient approach without significant efforts.

1.11.2 Mixed or Activity Coefficient-Based Approach

The mixed or activity coefficient approach uses the concept of activity coefficients to separate out the effects of nonideality because of component interactions and the effect of pressure. For the activity coefficient approach, we can rewrite the general equilibrium statement as

$$y_i \varphi_i^V P = x_i \gamma_i \varphi_i^{\text{SAT}} P^{\text{SAT}}(T) \text{PF}_i \quad (1.53)$$

$$\text{PF}_i = \exp \left(\int_{P^{\text{SAT}}}^P \frac{V_i(T, \pi)}{RT} d\pi \right) \quad (1.54)$$

In the equations, y_i is vapor molar composition of component i , φ_i^V is the vapor phase fugacity coefficient for component i , P is the system pressure, x_i is the liquid molar composition of component i , φ_i^{SAT} is the fugacity coefficient for vapor

pressure of component i , $P^{\text{SAT}}(T)$ is the vapor pressure of component i , and PF_i is the Poynting factor for component i at pressure P . V_i is the molar volume of component i as a function of temperature, T , and pressure, π (integrated from P^{SAT} to P). The PF_i factor is generally close to a value of 1 unless the system pressure is very high [17]. We can now rewrite the equilibrium relationship in the form of K -values as Eq. (1.55).

$$K_i = \frac{y_i}{x_i} = \frac{\gamma_i \varphi_i^{\text{SAT}} P^{\text{SAT}}(T)}{\varphi_i^V P} \quad (1.55)$$

We apply the Redlich–Kwong (RK) EOS [6] and liquid phase correlation (or an EOS) to obtain expressions for φ_i^V and φ_i^{SAT} as function of temperature, pressure, and component critical properties. This is the approach taken by the very popular Chao–Seader and Grayson–Streed methods [6]. The only factor that remains undefined is the liquid activity coefficient. The Chao–Seader and Grayson–Streed methods use regular solution theory to obtain an expression for γ_i as follows:

$$\ln \gamma_i = \frac{V_i}{RT} (\delta_i - \bar{\delta}) \quad (1.56)$$

$$\bar{\delta} = \frac{\sum x_i V_i \delta_i}{\sum x_i V_i} \quad (1.57)$$

where V_i is the liquid molar volume of component i and δ_i is the solubility parameter for component i . Molar volumes for pure components are readily available and we discussed several methods to estimate molar volumes for pseudocomponents in Section 1.10.5. We can obtain the solubility parameter for pseudocomponents using Eq. (1.56), where ΔH_{VAP} is the heat of vaporization, R is the universal gas constant, and T is system temperature. We have discussed how to calculate the heat of vaporization for pseudocomponents in Section 1.11.

$$\delta_i = \left(\frac{\Delta H_{\text{VAP}} - RT}{V_i} \right)^{0.5} \quad (1.58)$$

We use the K -value expression to calculate various equilibrium properties and perform typical process modeling flashes. As with the simple thermodynamic approach, we can use the heat capacities and heats of vaporization to obtain enthalpy balances for vapor and liquid streams. In addition, as we account for vapor and liquid phase nonideality due to component interaction, and temperature and pressure effects, we can also apply standard thermodynamic relationships to compute excess properties for enthalpies, and so on. The excess properties account for deviation of ideal mixing behavior and resulting deviations in equilibrium behavior.

Using the activity coefficient approach in the form of the Chao–Seader or Grayson–Streed method for refinery modeling is a significant improvement over the simple approach. The activity coefficient approach accounts for vapor and liquid phase nonidealities accurately in both the equilibrium and the enthalpy calculations. In addition, this approach is easy to integrate with other types of activity coefficient models that we may use in refinery models (especially for

sour water systems). We prefer to use activity coefficient models while dealing with heavy components that occur especially in vacuum distillation systems. A key shortcoming of this approach is that light components may require fictitious solubility parameters fitted to certain data sets and performance of this approach degrades quickly near the vicinity of the critical point. In general, however, this method is a reasonable thermodynamic model for real and pseudocomponents that we find in refinery reaction and fractionation systems.

1.11.3 Equation-of-State Approach

The most rigorous approach is the EOS approach. When we use an EOS, both vapor and liquid phases use the same model. We do not modify the general equilibrium statement from Eq. (1.50) because we can calculate the fugacity coefficients directly after we choose a particular EOS.

There are many types of EOS with a wide range of complexity. The RK model is a popular EOS that relies only on critical temperatures and critical pressures of all components to compute equilibrium properties for both liquid and vapor phases. However, the RK EOS does not represent liquid phases accurately and is not widely used, except as a method to compute vapor fugacity coefficients in activity coefficient approaches. On the other hand, the Benedict–Webb–Rubin–Starling (BWRS) EOS [6] has up to 16 constants specific for a given component. This EOS is quite complex and is generally not used to predict properties of mixture with more than few components.

For the purposes of refinery reaction and fractionation modeling, the most useful EOS models derive from either the Peng–Robinson (PR) EOS [6] or the Soave–Redlich–Kwong (SRK) EOS [6]. Both the PR and SRK are examples of cubic equations of state. Cubic EOSes are quick and easy to use for modeling work and provide a good balance between thermodynamic robustness and prediction accuracy. In our work, we have used the PR EOS with good results throughout many reaction and fractionation processes in refineries. More advanced EOS models are available in the context of refinery modeling, but we limit the scope of our discussion to the PR EOS.

We give the basic form of the PR EOS in Eq. (1.65). The PR EOS requires three main properties: critical temperature, critical pressure, and acentric factor.

$$a_i = 0.45724R^2 \frac{T_{ci}^2}{P_{ci}} \quad (1.59)$$

$$b_i = 0.07780R \frac{T_{ci}}{P_{ci}} \quad (1.60)$$

$$\alpha_i = [1 + (0.37464 + 1.5426\omega_i - 0.26992\omega_i^2)(1 - T_{ri}^{0.5})]^2 \quad (1.61)$$

$$a\alpha_{\text{MIX}} = \sum \sum x_i x_j (a\alpha)_{ij} \quad (1.62)$$

$$b_{\text{MIX}} = \sum x_i b_i \quad (1.63)$$

$$a\alpha_{ij} = \sqrt{a\alpha_{ii} a\alpha_{jj}} (1 - k_{ij}) \quad (1.64)$$

$$P = \frac{RT}{V_{\text{MIX}} - b_{\text{MIX}}} - \frac{a\alpha_{\text{MIX}}}{V_{\text{MIX}}^2 + 2b_{\text{MIX}}V_{\text{MIX}} + b_{\text{MIX}}^2} \quad (1.65)$$

where V_{MIX} is the molar volume of the mixture and k_{ij} is an interaction parameter for each i and j pair of components. The critical properties and interaction parameters for a large number of pure components are available within most process modeling software. We discussed how to obtain the critical properties of pseudocomponents in Section 1.10.4. In general, we can set the interaction parameters for pseudocomponents to 0 without significantly changing model results. Riazi [4] discussed several correlations to estimate the interaction parameters as functions of critical volumes of the components.

The EOS approach is robust and can generate the vapor pressure, heat of vaporization, liquid density, and liquid heat capacity using standard thermodynamic relationships and basic information such as critical properties and ideal gas heat capacities for all components. We refer the reader to the excellent text by Poling *et al.* [17] where there are detailed formulas for all these derived properties from the EOS directly. In general, the PR EOS makes good predictions of equilibrium distributions for light and medium boiling components. In addition, we ensure thermodynamic consistency by design as we use the same model for the vapor and liquid phases. The PR EOS also generates mostly acceptable predictions for vapor and liquid enthalpies and displays good behavior near the critical point.

A key shortcoming in the EOS approach (specifically PR) is that predictions of liquid density are quite poor and not sufficient for process modeling. The most popular method to deal with this problem is to ignore liquid density prediction from the EOS and use COSTALD method described in Section 1.10.5 to provide accurate density predictions. With similar reasoning, some process modeling software programs replace the enthalpy methods of EOS with Lee–Kesler correlations for heat capacity and enthalpy. However, this is not entirely necessary given the inaccuracies in the pseudocomponent physical property predictions themselves. Finally, the presence of very light components such as hydrogen and helium can sometimes provide spurious results. Aspen HYSYS includes several modifications (shown in Figure 1.58) for light components to prevent undesired behavior of light components. In general, we recommend using the EOS approach when developing refinery reaction and fractionation process models.

1.12 Miscellaneous Physical Properties for Refinery Modeling

In addition to thermophysical properties required for modeling purposes, a complete model must also make predictions regarding several fuel properties routinely measured at the refinery. Typically, these fuel or product properties include measurements such as flash point, freeze point, cloud point, and PNA content. These properties not only serve as indicators of product quality and distribution but may also be limited by government or internal refinery regulations. We can often justify the use of process modeling in the refinery by making sure that models also include predictions of these useful fuel properties. We will briefly discuss two approaches in this area and give concrete examples with flash point, freeze point, and PNA content. We choose these particular properties because

they display characteristics common to many types of fuel property correlation methods. We refer the reader to API standards [2] and Riazi [4] for more detailed expositions on various types of correlations for fuel properties not discussed in this section.

1.12.1 Two Approaches for Estimating Fuel Properties

Fuel or product properties can be a complex function of feed composition, process conditions, and analysis method. It is generally not possible to take into account all of these variables when estimating fuel properties.

The simplest approach is to correlate the relevant fuel property against modeled or measured bulk properties. For example, the flash point maybe correlated with the 10% point of the ASTM-D86 curve. We can obtain the required distillation curve from the pseudocomponent stream composition. The software accomplishes this task by arranging pseudocomponents in an ascending order of boiling point and creating a running cumulative sum of the liquid fractions of these pseudocomponents. This process results in the TBP curve of a given stream. Most software programs (including Aspen HYSYS) include methods to automatically convert this TBP curve into ASTM D86 or D1160 curve. Once we obtain this distillation curve, we can use several correlations to estimate flash point, freeze point, and so on. This method is simple to use and adaptable to any process simulator. However, this method relies on the availability of good correlations. It is important to remember that such correlations may not be valid or accurate for refineries that process frequently changing feedstocks.

A second approach is to use indexes based on pseudocomponent compositions. In an index-based approach, we represent each fuel property using the following equation:

$$\text{PROP}_{\text{MIX}} = \sum_{i=0}^N \text{PROP}_i w_i \quad (1.66)$$

where PROP_{MIX} represents a given fuel property; PROP_i represents the property index for pseudocomponent i ; w_i corresponds to the liquid, molar, or weight fraction; and N is the total number of pseudocomponents. Process modeling software tools and the literature have used this approach to quantify fuel properties such as octane numbers. An important advantage of this approach is that we can tune the property prediction to a particular plant by modifying the value of PROP_i . This allows the model user to track plant performance accurately. This method is also very useful while attempting to correlate the flash point of various blends of fuels. However, this approach is generally not portable across various process modeling software programs and requires a large initial data set to regress starting values for PROP_i . In addition, there is a danger of overfitting these values to match plant performance. Overfitting the property indexes renders the model less useful for predictive purposes. In our work, we have used both approaches with equal success. However, for simplicity, we recommend the first approach; especially in light of the fact that large sets of data may not be available for determining initial PROP_i values.

1.12.2 Flash Point

The flash point of a fuel typically refers to the temperature at which the fuel can ignite in the presence of an ignition source and sufficient air. A low flash point is an important consideration for gasoline engines as “sparking” or igniting the gasoline fuel is critical to optimum engine performance. In contrast, engines that use diesel and jet fuels do not rely on ignition (but on compression) and require fuels with a high flash point. The API [2] has correlated numerous data for a variety of fuels and found that the open- and closed-cup flash points (alternative measurement methods) linearly correlate well with the 10% ASTM-D86 distillation temperature.

The flash point correlation is

$$FP = A(D86_{10\%}) + B \quad (1.67)$$

where FP is the flash point measured in degree Fahrenheit and $D86_{10\%}$ refers to the 10% distillation temperature measured in degree Fahrenheit. A and B are specific constants for various feed types. Typical values of A and B are 0.68–0.70 and 110–120, respectively. We recommend performing a simple linear regression to tune existing measurements into this correlation. API notes that this correlation may be improved using the 5% distillation temperature instead of the 10% distillation temperature. Deviations of 5–7 °F are within the tolerance of this correlation.

1.12.3 Freeze Point

The freeze point refers to the temperature at which solid crystals start to appear as a given fuel sample is being cooled. The freeze point dictates how a given fuel may be sold and if additives or blendings are required to ensure that the fuel does not clog engines at low ambient temperatures. A related concept is the cloud point, which is the temperature at which the sample takes a cloudy appearance. This is due to the presence of paraffins, which solidify at a higher temperature than other components. The freeze point and cloud point do not correlate well with each without considering the paraffin content of the stream. The API [2] has correlated freeze point as follows:

$$FRP = A(SG) + B(K_w) + C(\text{MeABP}) + D \quad (1.68)$$

where FRP is the freeze point in degree Fahrenheit, SG is the specific gravity, K_w is the Watson K factor, and MeABP refers to the mean average boiling point. A , B , C , and D refer to specific constants for a given fuel composition. Typical values for A , B , C , and D are 1830, 122.5, -0.135 , and -2391.0 , respectively. We can also fix the value of K_w to a constant (roughly 12) for narrowly distributed petroleum cuts. We can calculate the value of MeABP using the spreadsheet procedure described in Section 1.4. It is important to compare this correlation to that for the flash point. This correlation uses more bulk measurements (SG and K_w) to capture the effect of feed composition on the freeze point.

1.12.4 PNA Composition

The last sets of correlations we discuss are composition correlations. These correlations identify chemical composition in terms of total PNA content of a particular feed based on key bulk measurements. These correlations are useful in two respects. First, we use these correlations to screen feeds to different refinery reaction units. For example, we may wish to send a more paraffinic feed to a reforming process when we need to increase the yield of aromatic components from the refinery. Second, these types of correlations form the basis of more detailed lumping for kinetic models that we discuss in detail in subsequent chapters of this book. We use these types of correlations to build extensive component lists that we can use to model refinery reaction processes.

Compositional information is quite useful to the refiner, and many correlations are available in the literature that attempt to correlate PNA content with various bulk measurements. In general, these correlations rely on density or specific gravity, molecular weight, distillation curve, and one or more viscosity measurements. The $n-d-M$ (refractive index, density, and molecular weight) [1], API/Riazi–Daubert [2, [4]], and TOTAL [19] correlations are just a few of the correlations available. The Riazi–Daubert correlation relies on the most directly observed information and we expect it to show the smallest deviation from measured values. The other correlations require parameters (aniline point, etc.) that may not be routinely measured for all feeds. The Riazi–Daubert correlation takes the form

$$\%X_P \text{ or } \%X_N \text{ or } \%X_A = A + B \cdot R_i + C \cdot VGC' \quad (1.69)$$

where $\%X$ represents the percent molar or volumetric composition of paraffins, naphthenes, or aromatics (based on the subscript chosen); R_i is the refractive index; and VGC' is the viscosity gravity constant or viscosity gravity factor defined in ASTM D2501-14. Coefficients A , B , and C take on different values based on whether an aromatic, naphthene, or paraffin is chosen as the subscript. This correlation can provide reasonably accurate results when we know the values of key input parameters with high accuracy. Overall, this method indicates a 6–7% absolute average deviation (AAD) from known measurement test cases.

We have extended the correlation by Riazi [1] to include the specific gravity, refractive index, and the stream viscosity. Our updated correlation is given by

$$\%X_P \text{ or } \%X_A = A + B \cdot SG + C \cdot R_i + D \cdot VGC' \quad (1.70)$$

$$\%X_N = 1 - (X_P + X_A) \quad (1.71)$$

In the equations, $\%X$ represents the percent molar or volumetric composition of paraffins (P), naphthenes (N), or aromatics (A) (based on the subscript chosen); SG is the specific gravity; R_i is the refractive index; and VGC' is the viscosity gravity constant or viscosity gravity factor. In addition, the constants A to D are given for paraffins and naphthenes and for each fuel type. We list our updated constants in Tables 1.6 and 1.7. We also group the constants in this updated correlation by boiling point ranges (light naphtha, etc.). This correlation reproduces plant data with 3–4% AAD, which is a significant improvement over the Riazi–Daubert

Table 1.6 Coefficients for paraffin content in petroleum fractions.

Boiling point range	Paraffin (vol%)				AAD
	A	B	C	D	
Light naphtha	311.146	-771.335	230.841	66.462	2.63
Heavy naphtha	364.311	-829.319	278.982	15.137	4.96
Kerosene	543.314	-1560.493	486.345	257.665	3.68
Diesel	274.530	-712.356	367.453	-14.736	4.01
VGO	237.773	-550.796	206.779	80.058	3.41

Table 1.7 Coefficients for aromatic content in petroleum fractions.

Boiling point range	Aromatic (vol%)				AAD
	A	B	C	D	
Light naphtha	-713.659	-32.391	693.799	1.822	0.51
Heavy naphtha	118.612	-447.589	66.894	185.216	3.08
Kerosene	400.103	-1500.360	313.252	515.396	1.96
Diesel	228.590	-686.828	12.262	372.209	4.27
VGO	-159.751	380.894	-150.907	11.439	2.70

correlation. We show how the grouping constants by boiling point ranges can be useful while creating kinetic lumping procedures for the FCC in Chapter 4.

1.13 Conclusion

This chapter discusses several key modeling steps regarding the characterization and the thermophysical properties of crude oil and petroleum fractions. The basic process for developing a set of pseudocomponents for modeling refinery fractionation systems is as follows:

- 1) The feed to the fractionation system is often poorly defined in terms of actual components. We may only have an assay and associated bulk property measurements (such as density). We use the techniques discussed in Sections 1.1.1–1.4 to produce a complete TBP distillation curve and a density or specific gravity distribution.
- 2) Once we obtain the TBP and density curve, we can cut the components into a number of pseudocomponents. Each of these pseudocomponents has at least a TBP and a density, by definition. The number of pseudocomponents for each cut point range can vary depending on the product range of the fractionation system. We have suggested the number of pseudocomponents for a few product ranges in Table 1.2. Subsequent chapters include more information for specific fractionation systems.

- 3) After obtaining the pseudocomponents, we decide how to model key physical properties (Section 1.10.1) for these components. Process modeling software often includes a large variety of correlations and estimation methods. However, for almost all cases, the Lee–Kesler correlations for critical properties and ideal gas heat capacities are sufficient. We have used the extended Twu correlation for molecular weight in our work. After obtaining the critical properties and molecular weight for a given pseudocomponent, we may estimate all other required properties (heat capacities, etc.) with correlations given by Riazi [1].
- 4) We also select a thermodynamic model to represent vapor–liquid equilibrium for these pseudocomponents. For crude fractionation columns, an EOS approach yields good results. However, an EOS approach does not predict liquid densities accurately and tends to give poor equilibrium predictions of heavy pseudocomponents. We can improve the EOS density predictions with more accurate density correlations such as COSTALD, Eq. (1.25). If the feed and products contain significant amounts of heavy products, it may be better to rely on empirical thermodynamic models such as Grayson–Streed or BK-10.
- 5) Lastly, we must make sure to use the product pseudocomponent information to verify measured product properties. In this chapter, we discuss the flash point, freeze point, and chemical composition properties of the products. The reader may find additional correlations for other fuel properties from the API handbook [2] and work by Riazi [1].

Although this chapter has focused extensively on the requirements for modeling fractionation systems, we can use the same techniques in the context of modeling refinery reaction process as well. We illustrate this process in Chapters 4–7. It is possible to obtain good predictive results for fractionation systems provided we make reasonable choices for the thermodynamics and physical properties of the pseudocomponents involved.

Nomenclature

A, B, α, β	Fitting parameters for cumulative beta distribution
CP_{IG}	Ideal gas heat capacity, J/mol K
CP_L	Liquid heat capacity, J/mol K
δ	Solubility parameter, (J/cc) ^{0.5}
$\bar{\delta}$	Mean weighted solution solubility parameter, (J/cc) ^{0.5}
$D86_{10\%}$	10% ASTM D86 distillation point, °F
FP	Flash point, °F
FRP	Freeze point, °F
γ	Activity coefficient, unitless
ΔH_{VAP}	Heat of vaporization, J/mol
ΔH_{VAP}^{NBP}	Heat of vaporization at normal boiling point temperature, J/mol
K_i	K -value, ratio of y_i/x_i , unitless
K_w	Watson K factor, unitless

K_{avg}	Watson K factor, unitless
k_{ij}	Interaction parameter for component i and component j in PR EOS, unitless
MeABP	Mean average boiling point temperature, K
MW	Molecular weight, g/mol
P	Pressure, bar
P_c	Critical pressure, bar
P_r	Reduced pressure = P/P_c , unitless
P^{SAT}	Saturation or vapor pressure, bar
PF_i	Poynting correction factor, unitless
PROP _{MIX}	Mixture of indexed fuel properties
PROP _{i}	Fuel property index for a given component
φ_i^{V}	Vapor phase fugacity coefficient for component i
φ_i^{SAT}	Liquid phase fugacity coefficient corrected to saturation pressure for component i
φ_i^{L}	Liquid phase fugacity coefficient for component i
R	Universal gas constant, 8.315 J/mol K
T	Temperature, K
T_c	Critical temperature, K
T_r	Reduced temperature = T/T_c , unitless
T_b	Boiling point temperature, K
T_{br}	Reduced boiling point temperature = T_b/T_c , unitless
ρ_{L}	Liquid density, g/cc
ρ_P	Liquid density at pressure P , g/cc
ρ_P°	Liquid density at reference pressure P° , g/cc
R_i	Refractive index, unitless
SG	Specific gravity, unitless
V^{SAT}	Molar volume of saturated liquid, cc/mol
V_i	Molar volume of component i as a function of temperature and pressure, cc/mol
VGC'	Viscosity gravity constant or viscosity gravity factor, unitless
w_i	Weighting factor for property index mixing
% X_{P}	Molar or volumetric composition of paraffins
% X_{N}	Molar or volumetric composition of naphthenes
% X_{A}	Molar or volumetric composition of aromatics
x_i	Liquid phase composition of component i
y_i	Vapor phase composition of component i
Z_{RA}	Rackett parameter, unitless
ω	Acentric factor, unitless

Bibliography

- 1 Kaes, G.L. (2000) *Refinery Process Modeling. A Practical Guide to Steady State Modeling of Petroleum Processes*, The Athens Printing Company, Athens, GA.
- 2 Daubert, T.E. and Danner, R.P. (1997) *API Technical Data Book – Petroleum Refining*, 6th edn, American Petroleum Institute, Washington, DC.

- 3 Bollas, G.M., Vasalos, I.A., Lappas, A.A., Iatridis, D.K., and Tsioni, G.K. (2004) Bulk molecular characterization approach for the simulation of FCC feedstocks. *Industrial and Engineering Chemistry Research*, **43**, 3270.
- 4 Riazi, M.R. (2005) *Characterization and Properties of Petroleum Fractions*, 1st edn, American Society for Testing and Materials, West Conshohocken, PA.
- 5 Sanchez, S., Ancheyta, J., and McCaffrey, W.C. (2007) Comparison of probability distribution functions for fitting distillation curves of petroleum. *Energy & Fuels*, **21**, 2955.
- 6 Walas, S.M. (1985) *Phase Equilibria in Chemical Engineering*, Butterworth-Heinemann, Burlington, MA.
- 7 Chen, C.C. and Mathias, P.M. (2002) Applied thermodynamics for process modeling. *AIChE Journal*, **48**, 194.
- 8 de Hemptinne, J.C. and Behar, E. (2006) Thermodynamic modeling of petroleum fluids. *Oil and Gas Science and Technology*, **61**, 303.
- 9 Lee, B.I. and Kesler, M.G. (1975) A generalized thermodynamic correlation based on three-parameter corresponding states. *AIChE Journal*, **21**, 510.
- 10 Kesler, M.G. and Lee, B.I. (1976) Improve prediction of enthalpy of fractions. *Hydrocarbon Processing*, **55**, 153.
- 11 Twu, C.H. (1984) An internally consistent correlation for predicting the critical properties and molecular weights of petroleum and coal-tar liquids. *Fluid Phase Equilibria*, **16**, 137.
- 12 Rackett, H.G. (1970) Equation of state for saturated liquids. *Journal of Chemical and Engineering Data*, **15**, 514.
- 13 Yamada, T.G. (1973) Saturated liquid molar volume. The Rackett equation. *Journal of Chemical and Engineering Data*, **18**, 234.
- 14 Spencer, C.F. and Danner, R.P. (1972) Improved equation for the prediction of saturated liquid density. *Journal of Chemical and Engineering Data*, **2**, 236.
- 15 Thomson, G.H., Brobst, K.R., and Hankinson, R.W. (1982) An improved correlation for densities of compressed liquids and liquid mixtures. *AIChE Journal*, **28**, 671.
- 16 Cheuh, P.L. and Prausnitz, J.M. (1969) A generalized correlation for the compressibilities of normal liquids. *AIChE Journal*, **15**, 471.
- 17 Poling, B.E., Prausnitz, J.M., and O'Connell, J.P. (2000) *Properties of Gas and Liquids*, 5th edn, McGraw-Hill, New York.
- 18 Agarwal, R., Li, Y.K., Santollani, O., Satyro, M.A., and Vieler, A. (2001, May) Uncovering the realities of simulation. *Chemical Engineering Progress*, **42**.
- 19 Sadeghbeigi, R. (2000) *Fluid Catalytic Cracking Handbook. Design, Operation and Troubleshooting of FCC Facilities*, Gulf Publishing Company, Houston, TX.
- 20 Mohan, S.R. (2016) *Five Best Practices for Refineries: Maximizing Profit Margins through Process Engineering*, <https://www.aspentech.com/White-Paper-Five-Best-Practices-Refineries.pdf>.
- 21 Niederberger, N. (2009) *Modeling, Simulation and Optimization of Refining Processes*, <https://www.slideshare.net/Bioetanol/wks-biorefinery-jacques-niederbergerpetrobras-refino>.
- 22 Wu, Y. (2010) Molecular modeling of refinery operations. Ph.D. dissertation. University of Manchester, Manchester, United Kingdom, <https://www.escholar>

.manchester.ac.uk/api/datastream?publicationPid=uk-ac-man-scw:93706&datastreamId=FULL-TEXT.PDF.

- 23 Mullick, S., Dooley, K., Dziuk, S., and Ajikutira, D. (2012) *Benefits of Integrating Process Models with Planning and Scheduling in Refining Operations*, <https://www.scribd.com/document/269573466/Integrating-Process-Models-With-Refining-PandS>.
- 24 Aspen, Technology, Inc. (2012) *Molecule-Based Characterization Methodology for Correlation and Prediction of Properties for Crude Oil and Petroleum Fractions* (Molecular Characterization White Paper), https://origin-www.aspentech.com/Molecular_Characterization_White_Paper.pdf.